Journal of *Marine Science and Engineering*

MDPI

Article

Nearshore Migration of Munitions and Canonical Objects Under Large-Scale Laboratory Forcing

Temitope E. Idowu [1,*], Emily Chapman [2], Manoj K. Gangadharan [3], Jacob Stolle [4] and Jack A. Puleo [1,*]

[1] Center for Applied Coastal Research, University of Delaware, Newark, DE 19716, USA
[2] Stantec Engineering Consultants, New York, NY 10017, USA; emily.chapman@stantec.com
[3] WSP Canada Inc., Vancouver, BC V6Z 2M1, Canada; manojkumar.gangadharan@wsp.com
[4] Environmental Hydraulics Laboratory, Institut National de la Recherche Scientifique, Québec City, QC G1P 4S5, Canada; jacob.stolle@inrs.ca
* Correspondence: teidowu@udel.edu (T.E.I.); jpuleo@udel.edu (J.A.P.)

Abstract: A quantitative understanding of the migration of munitions and canonical objects in the nearshore is needed for the effective management of contaminated sites. Migrations of munitions with a density range of 2000 kg/m^3 to 5720 kg/m^3 were quantified in a large-scale wave flume. The forcing consisted of six cases of varying wave heights, periods, still water depths, and durations. The cross-shore profile, typical of natural sandy beaches, was sub-divided into swash, surf, and offshore zones. Overall, 2228 migration measurements were recorded with 16% and 84% of the migration observations classified as "motion" (net distance > 0.5 m) and "no motion" (net distance $\leq$ 0.5 m), respectively. The probability of munitions migration increased with proximity to the shoreline. There was a nearly equal probability of onshore or offshore migration in the swash zone. Migration in the surf zone tended to be offshore-directed (65%), while migration was onshore-dominant (65%) in the offshore zone. Migration in the offshore zone was preferentially onshore due to skewed waves over flat bathymetry. Less dense munitions in the offshore zone may have migrated offshore likely still related to the skewed nature of the wave profile causing transport in both directions through the majority of the wave phase. The largest migration distances occurred in the surf zone likely due to downslope gravity. Migration in the surf and swash zones is a balance between skewed/asymmetric forcing and downslope gravity, with downslope gravity tending to be pronounced provided the forcing is sufficient to initiate motion. An exception was sometimes observed in the swash zone where onshore forcing was sufficient to transport munitions to the seaward side of the berm where they became trapped in a bathymetric depression between the dune and berm. Relating overall migration (Lagrangian) to fixed hydrodynamic measurements (Eulerian) was ineffective. Parameters such as the Shields number, wave skewness, and wave asymmetry estimated from the closest measurement location were insufficient to predict migration. Large scatter in the migration data resulting from competing hydrodynamic, morphodynamic, and munitions response processes makes robust deterministic predictions with flow statistics and dimensionless numbers difficult.

Keywords: munitions; unexploded ordnance; solid objects; migration; nearshore

Citation: Idowu, T.E.; Chapman, E.; Gangadharan, M.K.; Stolle, J.; Puleo, J.A. Nearshore Migration of Munitions and Canonical Objects Under Large-Scale Laboratory Forcing. *J. Mar. Sci. Eng.* **2024**, *12*, 2103. https://doi.org/10.3390/jmse12112103

Academic Editor: Francesca De Serio

Received: 23 October 2024
Revised: 13 November 2024
Accepted: 15 November 2024
Published: 20 November 2024

1. Introduction

Munitions or unexploded ordnance (UXO) are ammunitions belonging to a larger family of explosives. Munitions existing in the environment consist of ordnance that failed to detonate as intended, functioned as intended but harbor residual explosive or potentially active chemical warfare agents, were discarded, broken-down, or abandoned, or are dummy rounds [1]. Widespread munition disposal at sea was a prevalent practice from the late 1800s until the 1970s, at which point international conventions were enacted to bring an end to the practice [2]. The aftermath of ocean disposal of munitions is a global concern currently impacting over 40 countries [2]. The quantity of munitions present in the

oceans remains uncertain due to limited documentation. However, conservative estimates suggest that at least 1.6 million tons of chemical weapons munitions were disposed of in the oceans [3]. In the United States alone, more than 70 chemical weapons and munitions disposal events occurred in coastal waters between 1918 and 1970. There are more than 10 million acres across over 400 designated sites possibly containing munitions in underwater environments within the Formerly Used Defense Sites program alone [4,5]. The reappearance of underwater munitions occurred in the Gulf of Mexico and along the coastlines of at least 16 states [6].

Nearshore hydrodynamic and morphodynamic processes can lead to munitions burial, migration, and/or exposure. The latter two processes are of particular concern near the shoreline, posing a public risk. Some previous field and laboratory studies expanded knowledge on munitions/munition-like object behavior in the underwater environment [7–10]. Near instantaneous measurements have been used to quantify boundary layer processes that lead to burial and migration at high spatial and temporal scales under field conditions [7]. Laboratory experiments have been used to improve understanding of the transport, fate, and phenomenology of munitions on hard-bottom substrates [8] and munitions behavior including incipient motion, scour burial processes, and obtaining power law relationships between munitions critical object mobility and the diameter to bottom roughness [10]. Other studies occurred on the behavior of munitions/munition-like objects in the nearshore [11–13] shoaling zone under nonlinear progressive waves [14], and the swash zone under dam-break forcing [15–18]. These studies provided descriptive and probabilistic insights into the behavior of munitions under different forcing conditions. Several studies attempted to develop empirical relationships for migration and burial [13,19–21]. Migration predictions are more difficult due to additional hydrodynamic processes such as wave breaking and pressure gradients with correlation coefficients between forcing and response of below 0.4 [13].

Morphodynamics can lead to munitions burial or exposure. For instance, munitions appeared after storm events either transported from offshore regions, exhumed via sediment erosion, or brought onshore as dredged material [22–24]. Recent studies show that more dense munitions experienced little or no migration [13,15,16,18]. However, the bulk density parameter space in these prior studies was limited, necessitating more detailed migration studies [13].

Predicting munitions migration is difficult due to complex, interrelated processes of hydrodynamics, morphodynamics, grain-scale processes, and munitions characteristics [25]. Aspects of the complex interactions and force balance on a submerged object have been described mathematically [10,12,26,27], but are generally related to the initiation of motion rather than migration distance. Lacking proper deterministic relationships, empirical and other models have been used for improving munitions migration prediction. However, due to the highly stochastic nature of munitions behavior, comprehensive experimental data are needed for creating data-driven predictions [28] and for validation of coupled probabilistic or computational models [26,29–31]. The Underwater Munitions Expert System (UnMES; [31]), a Bayesian expert system, requires a broad data set for training and testing. Limited validation of UnMES has been completed based on available data, but predictive skill was moderate with existing migration distance data especially closer to the shoreline [32,33]. The Munitions Response Library (MRL) is a robust community standard repository that aggregates information related to munitions behavior and uses UnMES in a predictive approach [25,34] currently focusing outside the shoaling zone. More robust data from the shoaling zone landward are needed to train UnMES and enhance the MRL. Ultimately, the data-driven framework and repository will form an integral part of the munitions mobility and burial reference manual that aims to translate the science of munitions phenomenology into real-world munitions response site management [25].

This paper presents a comprehensive study on a range of munitions with bulk densities from 2000 kg/m^3 to 5720 kg/m^3, spanning simultaneously the swash, surf, and offshore zones. Surrogate munitions and canonical objects were deployed in a large-scale wave

flume on a mobile bed under different forcing conditions. The overarching objective is to quantify munitions migration in the different cross-shore regions in relation to bulk hydrodynamics and morphodynamics.

2. Experimental Setup and Operational Methods

2.1. Wave Flume and Conditions

The experiment was conducted in a large-scale wave flume (Figure 1) with a berm and dune beach profile typical of sandy beaches. An array of sensors was used to quantify flow conditions and morphodynamics. Munitions with bulk densities spanning 2000 kg/m^3 to 5720 kg/m^3 were placed at different cross-shore locations (stations) on the beach profile from offshore to the swash zone.

Figure 1. View of the INRS wave flume looking in the onshore direction.

The large-scale wave flume is 120 m long, 5 m deep, and 5 m wide, managed by the Environmental Hydraulics Laboratory, *Institut National de la Recherche Scientifique* (INRS), Quebec, Canada (Figure 2). The piston-type wave paddle with active absorption has a maximum stroke length of 4 m and 4 m/s maximum velocity. Wave flume water depth and wave period ranges of 2.5–3.5 m and 3–10 s, respectively, are possible [35]. The wave flume has a water transfer system connected to a reservoir with a capacity of 3500 m^3. Sediment with a median grain size (d_{50}) of 0.28 mm was available in the wave flume and from a nearby quarry.

The experiment consisted of six hydrographs (cases) with different rates of increasing intensities (Table 1) based on the maximum capabilities of the wave flume. Each case (except Case05) comprised five trials of irregular waves with varying trial durations, still water depths, peak wave periods (T_p), and significant wave heights (H_s). The trials in each case were such that the hydrodynamic conditions were ramped up from the first to the last trial. The minimum and maximum values of H_s, T_p, and still water depths were 0.21–1.4 m, 2.5–12 s, and 2.1–3.3 m, respectively. Three hundred irregular waves were forced in each trial using a TMA spectrum [36]. The beach profile was recreated in the wave flume for each case before the deployment of sensors and munitions.

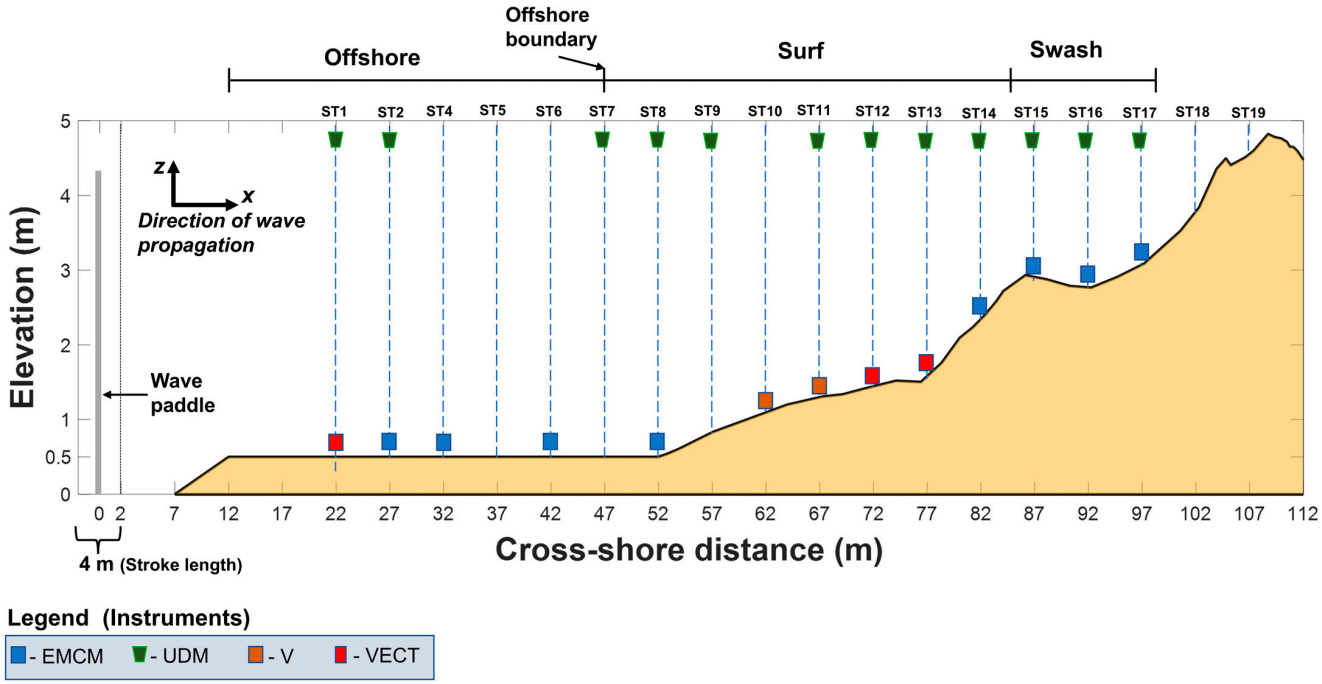

Figure 2. The beach profile showing the sensor layout and approximate zones of the nearshore. The dashed blue lines indicate the station locations.

Table 1. Hydrodynamics characteristics for the different Cases.

Case Number	Number of Trials	Still Water Depth (m)	Significant Wave Height H_s (m)	WavePeriodT_p (s)	Duration (hr)
01	5	2.1	0.72	7.11	0.59
02	5	2.87	1.1	6	0.50
03	5	3.3	1.4	6	0.50
04	5	2.23–2.87 Increment: 0.15–0.17	0.21–1.1 Increment: 0.22–0.23	2.54–5.99 Increment: 0.84–0.86	0.21–0.50 Increment: 0.07–0.08
05	10	2.24–2.87 Increment: 0.6	0.21–1.1 Increment: 0.09–0.1	2.54–5.99 Increment: 0.38–0.39	0.21–0.50 Increment: 0.03–0.04
06	5	2.23–2.87 Increment: 0.15–0.17	0.6	8–12 Increment: 1	0.67–1.00 Increment: 0.08–0.09

Case01 to Case03 had increasing still water depths and wave heights, and a wave onset of $^{dH_s}/_{dt} = \infty$; where *dt* is the time increment between the H_s values of two successive trials, meaning the largest waves were forced from the first trial on. Case04 and Case05 maximized wave height as still water depths increased with each trial. However, Case04 had a faster wave onset, $^{dH_s}/_{dt} = 15$ with 5 trials to reach the maximum H_s, while Case05 had a slower wave onset with $^{dH_s}/_{dt} = 7$ over 10 trials. Case06 focused on maximizing the wave period while maintaining a still water depth increase similar to Case04 but with a $^{dH_s}/_{dt} = \infty$.

2.2. Wave Flume Layout

The steps in the wave flume setup were: (1) marking the beach profile elevations on the wave flume sidewalls, (2) adding sediment using a bucket loader, (3) spreading and compacting the sediment to match the marked profile elevations, (4) installing galvanized pipes and scaffold frames at the different cross-shore stations for sensor installation, (5) routing sensor cables into the control trailer, (6) placing munitions at the different cross-shore stations, (7) conducting the case according to the prescribed hydrodynamic conditions, (8) periodic wave flume draining for profiling and munitions surveying, and (9) resetting the beach profile for the next case. The beach profile (Figure 2) spans approximately 60 m and includes an additional roughly 50 m flat section of 0.5 m depth of sand for a smoother transition from

the concrete flume bottom to the mobile bed of the actual profile. There are 18 cross-shore stations spaced 5 m apart and spanning from the dune face to the offshore zone (Figure 2). The at-rest position of the piston wavemaker sets the origin for cross-shore coordinate (x), increasing onshore. The vertical elevation, z, is positive up from the concrete bottom of the wave flume, and the alongshore coordinate, y, increases to the left for an observer looking onshore (right-handed coordinate system). The beach slope is gentler at about 1:20 from the flat section to x = 72 m and steeper at about 1:5 between x = 77 and x = 87 m of the scaled profile. Overall, the foreshore profile is relatively steep at about 1:14 (Figure 2).

Only sensors used in this paper are described. A total of 25 sensors comprising 2 Nortek Vectors (V), 3 Nortek Vectrino II Acoustic Doppler Profiling Velocimeters (VECT), 8 Valeport model 802 Electromagnetic Current Meters (EMCM), and 12 MassaSonic PulseStar M-300 Ultrasonic Distance Meters (UDM) were deployed. The V measures the three velocity components (u, v, and w) at a single elevation 0.15 m below the transducer. Vectors recording at 64 Hz were placed at stations 10 and 11 in the surf zone (Figure 2) at 0.25 m above the bed. The VECT measures the three velocity components (u, v, and w) over a 30 mm profile at 1 mm increments with the first bin beginning 0.04 m below the transducer. The VECTs recording at 100 Hz were placed at station 1 at 0.2 m above the bed and at stations 12 and 13 in the surf zone at 0.06 m above the bed. The EMCM measures the horizontal velocity (u, v) at a single elevation above the bed. The eight EMCMs recording at 16 Hz were placed at stations 2, 4, 6, 8 14, 15, 16, and 17 (Figure 2). EMCMS were placed at 0.1 m (offshore) and 0.06 m (surf and swash zone) above the bed. The UDM records the vertical distance from its position to the free surface or the bed. The UDMs were located at 12 of the 18 stations (Figure 2). Some data were missing because a few EMCMs or UDMs malfunctioned. All sensors were connected to recording laptop computers or computer-controlled data loggers. Computers were on a local network receiving clock updates every second via a Garmin GPS antenna and Tac32 and Dimension4 v5.3 software.

Pre- and post-trial elevations and munition locations were collected using a Leica global navigation satellite system (GNSS) real-time kinematic global positioning system (RTK GPS), a Trimble S5 total station, and a D710U sonar device from EchoLogger. The GPS and total station were used to take point measurements of the munition locations and beach profile (expected errors O(0.05 m)). The sonar was used for elevation measurements of the wet portions of the profile. GPS and total station data were merged with sonar elevations to create a beach profile. The northing, Easting, and elevation formats were then converted into the wave flume coordinates.

2.3. Surrogate Munitions, Canonical Objects, and Instrumentations

Munitions span a range of shapes, sizes, and bulk densities. Numerous studies employed basic cylindrical shapes and varying-sized conical frusta of various bulk densities as munition surrogates [7,8,10,14,21,28]. An overview of the various munitions-related studies and the physical characteristics of the objects used (diameter, length, and bulk density, ρ_m) can be found in [28]. Here, munitions ranging from 40 mm to 155 mm diameter (D) were deployed. Canonical objects (spheres and cylinders) were also used for simplicity in modifying bulk density. Recent prior studies developed replicas with similar shapes, sizes, geometrical characteristics, and bulk densities as real munitions within an acceptable absolute error of <20% [11,13]. In this study, canonical objects were fabricated using iron shavings mixed with leveling cement (spheres) or Quikrete concrete mix (cylinders; within aluminum tubes) to obtain desired densities. The target densities of the spheres were 2500 kg/m^3, 3000 kg/m^3, 3500 kg/m^3, and 4000 kg/m^3, while the target densities of cylinders were 2000 kg/m^3, 2500 kg/m^3, 3000 kg/m^3, and 3500 kg/m^3. The percent errors between the fabricated canonical objects and the target densities were within 7%. A total of 152 surrogate munitions and canonical objects were used (Figure 3). Three 81 mm projectiles with bulk densities of 2500 kg/m^3, 3000 kg/m^3, and 4180 kg/m^3 housed an x-IO inertia motion unit (IMU). The IMUs measure near-instantaneous motion including acceleration, angular velocity, and orientation. These 81 mm surrogates were deployed in the surf zone.

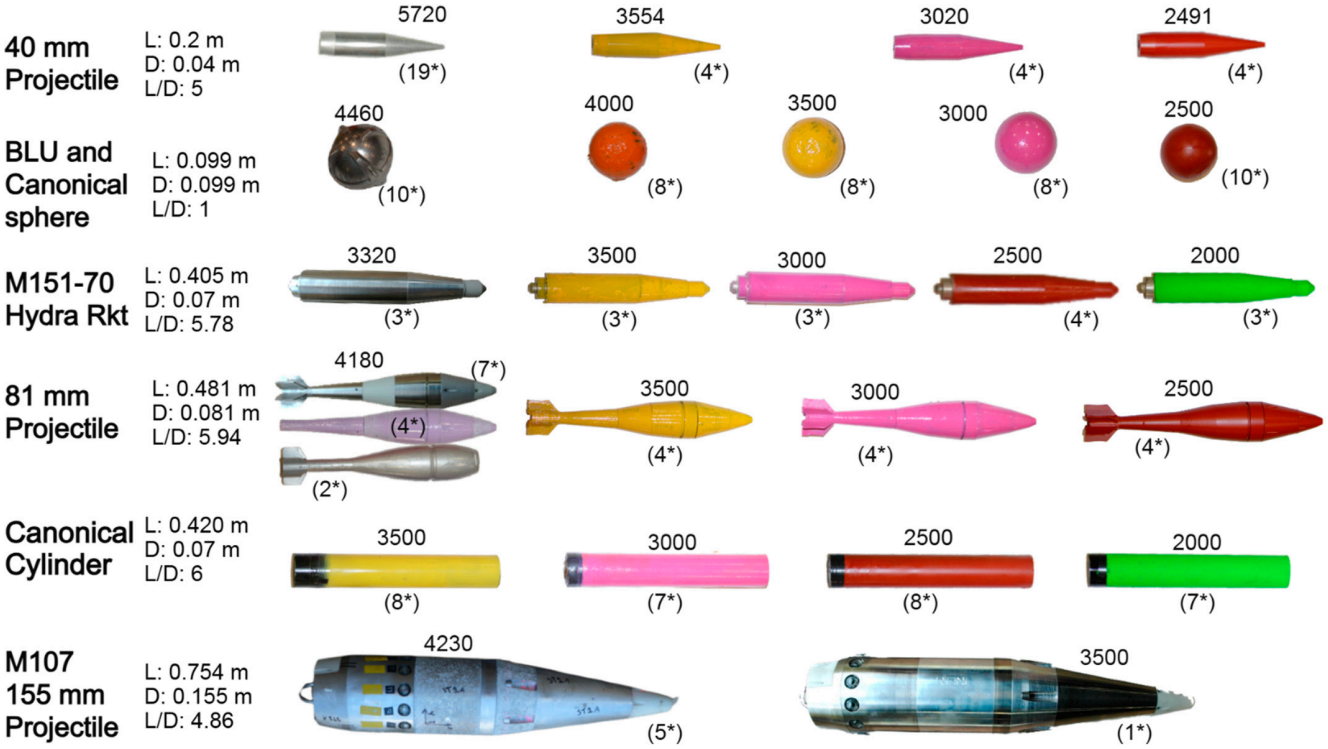

Figure 3. Range of characteristics of munition objects deployed, L is the object length, and '*' indicates the number of objects of a specific type deployed.

Instrumenting munitions with IMUs provided Lagrangian observations of munitions response to varied forcing conditions. The IMUs were inserted into and retrieved from the munitions before and after several trials. IMUs were set to sleep/wake mode, extending battery life by entering sleep after 60 s of inactivity. The trigger for wake-up was set to "high sensitivity" with a sample rate of 256 Hz. The principal measurements of the IMU are roll, angular velocity, and yaw. The roll measurements were converted into translational distance and by extension, the munition trajectories within the wave flume coordinates using a cumulative sum technique [13,37].

The total number of unique munitions bulk density used in the experiment was 13, although the total bulk density variations across all objects was 25 (Figure 3). To the authors' knowledge, this study comprises the largest collection and range of bulk density munitions deployed in a single study for quantifying munitions migration in the nearshore. Figure 3 highlights the munitions and canonical objects deployed in the study and the density range using color coding where green, red, magenta, and yellow were near 2000 kg/m^3, 2500 kg/m^3, 3000 kg/m^3, and 3500 kg/m^3, respectively. Gray/silver-colored objects retain their typical bulk density as identified by the SERDP standardized repository or military manuals [11]. When appropriate, these color codings are retained in the presentation of the results for direct correspondence.

3. Example Hydrodynamic and Morphodynamic Observations

Time series of water depth (h) and u (Figure 4) across the stations (Table 1) were time-synchronized. The data pre-processing involved resampling all datasets to 100 Hz, using a moving average filter to remove noise, and clipping out the relevant parts of the datasets that were within the duration of the actual forcing. Intermittent portions of the velocity time series where the beach profile was momentarily dry based on the depth information from the UDMs were removed. The velocity data were further quality-controlled by setting absolute velocity thresholds of 3 m/s and removing spikes with values larger than the threshold. Example time series data of the first 100 s of the h and u extracted from the largest forcing conditions (Case03 Trial01) are shown in Figure 4.

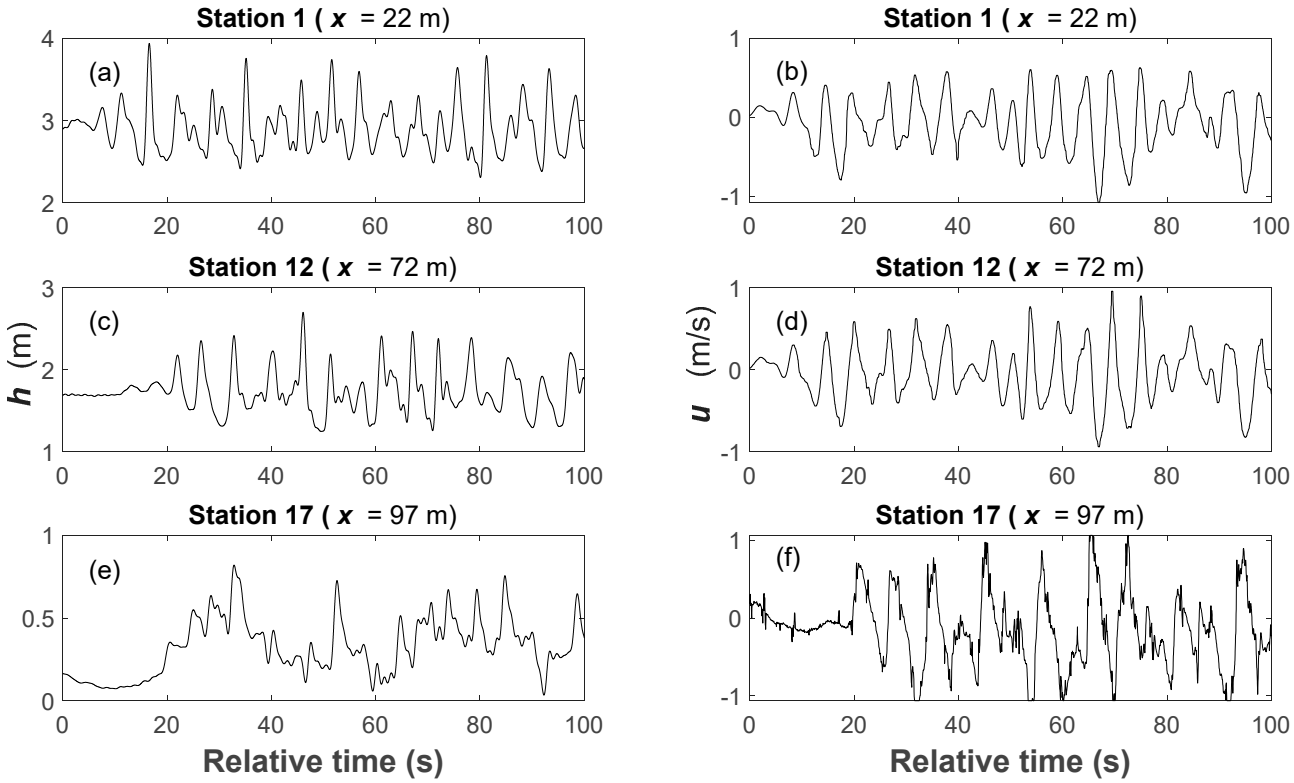

Figure 4. Time series excerpts of water depth (h) and cross-shore velocity (u) for the first 100 s of the largest forcing conditions (Case03, Trial 01) in the offshore (**a**,**b**), surf (**c**,**d**), and swash (**e**,**f**) zones.

The time series show a progressive decrease in h as waves propagate from the offshore to the swash zone (Figure 4). Breaking processes and bore capture led to fewer waves observed near the beach face compared to offshore (Figure 4). There is a transition to more skewed/asymmetric waves with a decrease in water depth (Figure 4b,d,f). Swash data are more sawtooth-shaped, as expected [38]. The profile contained a long flat section providing space for waves coming off the paddle to adjust to local water depth before shoaling on the actual profile. Still, the accommodation space may have been insufficient, causing alterations to the wave shape relative to expectations for the actual depth. It is believed these alterations are insignificant for the study of migration given the deployment of munitions across the profile.

Variations in bulk hydrodynamics H_{rms} and U_{rms} from the UDMs and velocity meters for all cases and trials are presented in Figure 5 (where rms is the root mean square). The H_{rms} was calculated assuming a Rayleigh distribution as a direct relationship with H_s as $H_{rms} = \frac{H_s}{\sqrt{2}}$, and H_s is estimated from the UDM data using the relationship $H_s = 4 * \sigma_h$, where σ_h is the standard deviation of the free surface oscillation. H_{rms} values tend to show a gradual progression with slight shoaling followed by breaking. Case04 and Case05 showed the widest variations in H_{rms} due to the progressive increase in H_s from 0.21 m to 1.1 m in both Cases. Breaking typically occurred near x = 77 m with variations depending on forcing conditions. Waves then dissipated across the remainder of the profile into the swash zone.

The U_{rms} were computed by obtaining the root mean square of the velocity time series. The U_{rms} values (Figure 5g–l) followed similar patterns with the H_{rms} observations. Velocities for Case01, Case02, and Case03 were nearly constant at around 0.4 m/s across the flat section; indicative of the wave field having adjusted to the local water depth. The similarity also suggests that for these trials, the wave height variability did not cause large variability in U_{rms}, likely due to a corresponding increase in still water depth. Case04 and Case05 did show a consistent increase in U_{rms} with respect to trial number as the wave height and period increased with the increasing still water depth. Case06 had the longest wave periods and fixed wave heights. Little variability in U_{rms} was observed in the flat

section, and magnitudes were smaller than for the first three Cases. For all Cases, U_{rms} were greatest following breaking and into the swash zone. These observations imply that erosion/accretion processes and near-bed forcing were more prominent in the inner surf and swash zones. Thus, migration processes may also be more prominent in these regions.

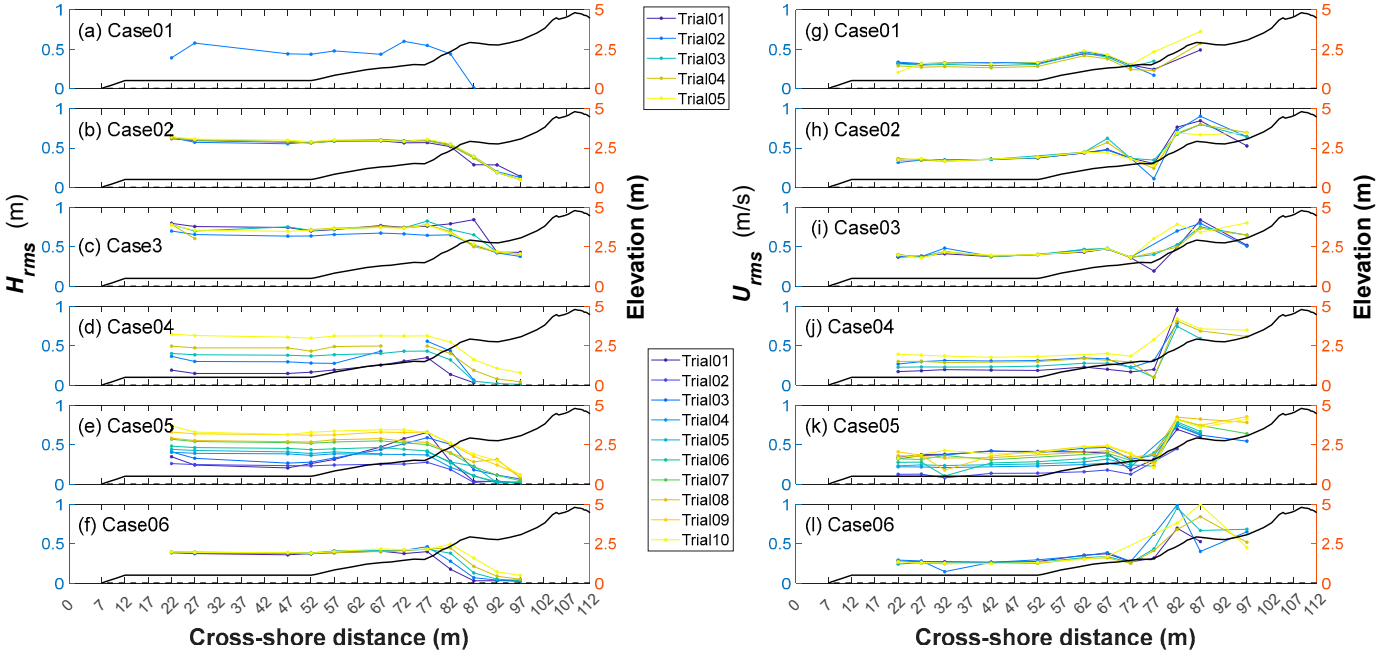

Figure 5. Cross-shore distribution of H_{rms} (**a**–**f**) and U_{rms} (**g**–**l**) for all Cases.

Temporal variability in beach profiles for Case03, as an example, shows the locations of erosion and accretion and variability in local beach slopes (Figure 6). The berm between x = 82 m and x = 90 m eroded offshore, causing accretion and sand bar formation between x = 76 m and x = 82 m (Figure 6). The sand bar shifted offshore as the trial sequence progressed and this motion was observed for many of the Cases.

The morphodynamics for all cases were analyzed by subtracting the beach profile measurements after each trial from the pre-trial measurements (Figure 7). Positive and negative values imply accretion and erosion, respectively. Across all Cases, minimal bed level changes (within the range of ± 0.1 m) were observed in the offshore zone to roughly x = 70 m. The small changes are likely due to sensor accuracy, weak sediment transport gradients, and variations in three-dimensional ripple formation and migration captured using a single cross-shore profile. From x = 70 m to x = 100 m, more substantial erosion/accretion to a magnitude of 0.4 m was observed (Figure 7). The region from x = 75 m to x = 90 m, where wave breaking was concentrated and with the steepest slope (1:5), experienced the most noticeable bed level changes. The bed level changes and morphodynamics observed across the cases vary from least to most severe as Case01, Case04, Case06, Case02, Case03, and Case05. Case01 had the smallest still water depth, and H_s, values of 2.1 m and 0.72 m, respectively (Table 1). Bed level changes were less than ±0.2 m even in the region between x = 70 m and x = 90 m, indicating little variability in the berm. Case04 had conditions of still water depth and H_s of 2.23–2.87 m and 0.21–1.1 m, respectively. Berm erosion and sand bar formation occurred between x = 80 m to x = 90 m and x = 75 m to x = 80 m, respectively. Case06 had a still water depth range of 2.23–2.87 m similar to Case04, but with a constant H_s of 0.6 m and longer wave periods. Unlike Case04, greater accretion occurred offshore of the erosion point between x = 75 m and x = 80 m and onshore between the x = 90 m and x = 100 m region coinciding with the dune toe. Case02 had a still water depth of 2.87 m and H_s =1.1 m values, leading to weaker accretion and greater erosion from x = 75 m to x = 80 m and x = 80 m to x = 90 m, respectively, than in Case06. Case03 had the largest still water depth and wave height combinations

(3.3 m and H_s = 1.4 m), resulting in extensive accretion and sand bar formation from x = 75 m to x = 80 m and corresponding erosion of the berm and dune toe. Case05 had the most substantial morphodynamics. The forcing combinations were similar to Case04 (Table 1), but the forcing ran over the course of 10 trials. The longer duration led to a greater magnitude of erosion and accretion relative to Case04.

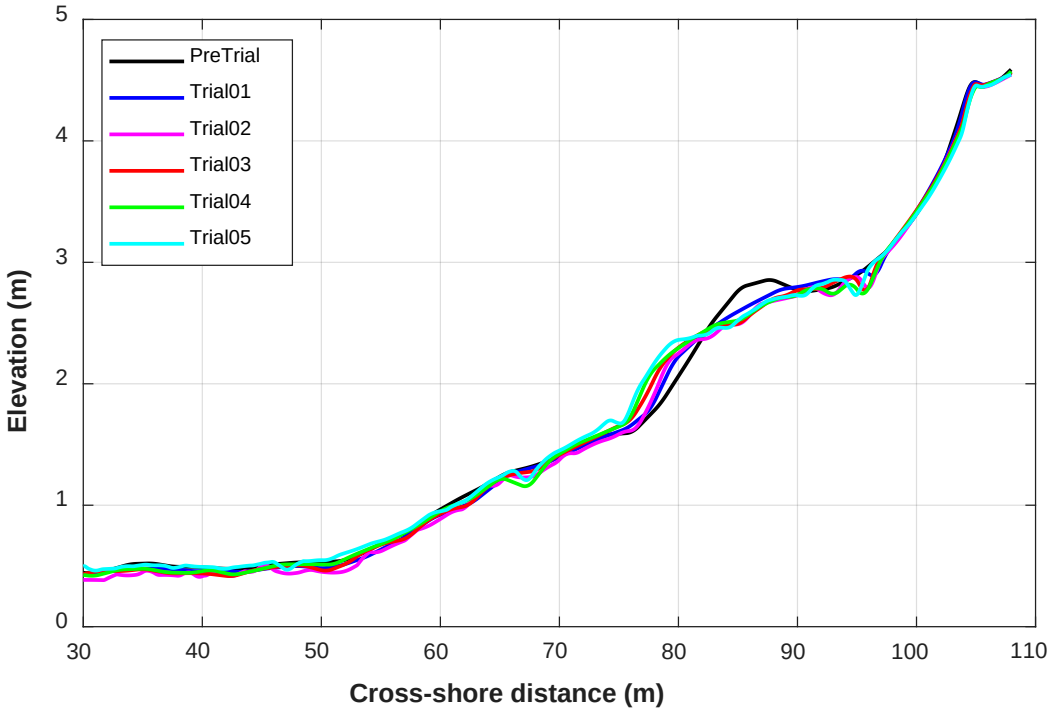

Figure 6. Beach profile measurements for Case03.

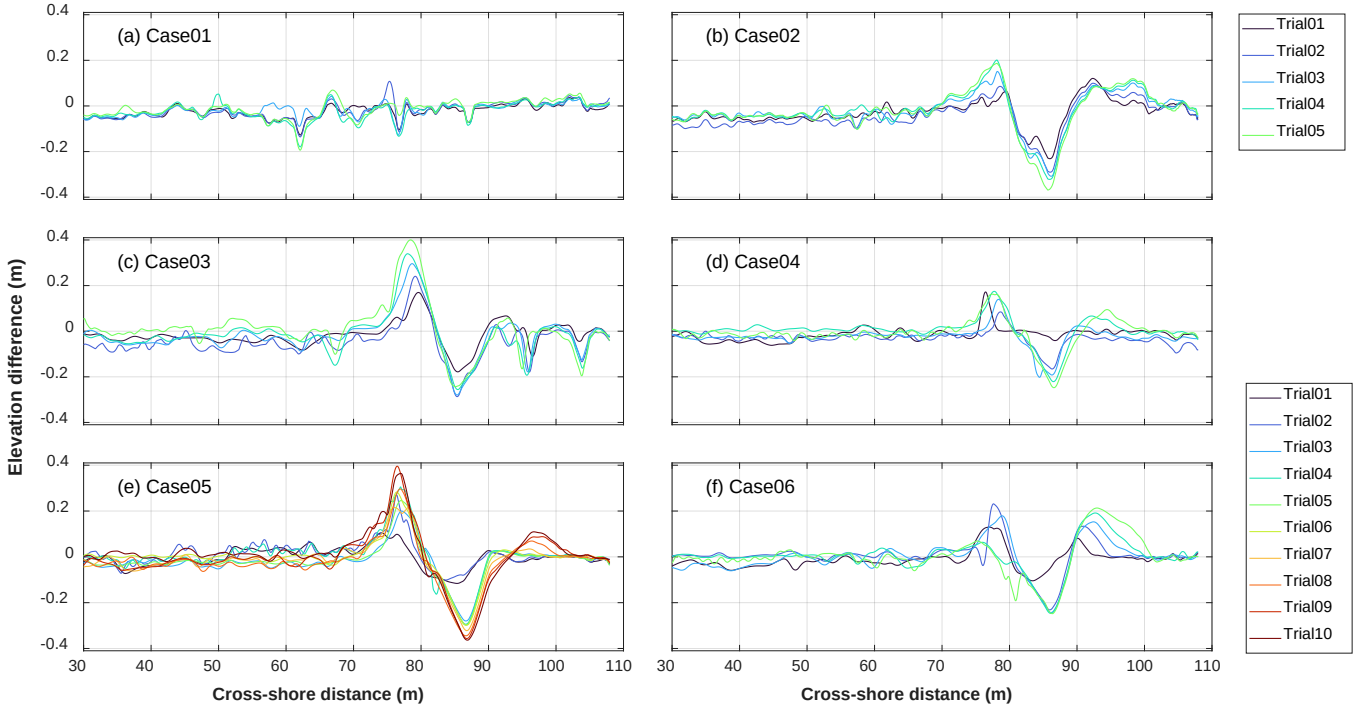

Figure 7. Changes in the beach profile elevation relative to the pre-trial elevation.

4. Results

4.1. Munitions Migration–Combined

Migration distances were subdivided into two categories: "no motion" for cross-shore migration magnitudes less than or equal to 0.5 m, and "motion" for cross-shore migration magnitudes exceeding 0.5 m. This threshold value was chosen based on roughly the longest dimension of the munitions that often experienced motion (mortars and rockets) and a desire to exceed expected measurement errors by an order of magnitude. Of the total 152 munitions deployed, 40 munitions (26%) were deployed initially in the offshore zone. The munitions deployed in the surf zone and swash zones varied from 42 to 55% and 19 to 32%, respectively. Munitions were surveyed before the first trial and generally after every other trial when the wave flume was drained. Generally, full surveys were achieved after Trials02, 04, and 05 in cases containing 5 trials, and in Case05 containing 10 trials, full surveys were achieved after Trials02, 04, 06, 08, and 10. Only partial surveys spanning the swash and shallow parts of the surf zone were achieved after the other trials. Some munitions could not be located due to extensive burial or being located underwater before wave flume draining. Munitions that were landward of the maximum runup and experiencing no hydrodynamic forcing were excluded from the data set. A total of 2228 migration measurements were obtained encompassing all cases and trials.

Data are presented in tabular form and as histograms (Table 2, Figure 8) with the color-coding separating munitions by specific gravity (SG) and matching the munitions colors provided in Figure 3. Negative and positive migration values imply offshore and onshore migration, respectively. The "motion" and "no motion" migration observations were 349, and 1879, respectively, implying that 84% of the deployed munitions did not migrate beyond 0.5 m of their initial location. The percentages of the "no motion" munitions (Figure 8a) with SG ranges of $2 \leq SG < 2.5$, $2.5 \leq SG < 3$, $3 \leq SG < 3.5$, $3.5 \leq SG < 4$, $4 \leq SG < 4.5$, and $4.5 \leq SG < 5.8$ were 8% (152), 17% (317), 19% (357), 21% (391), 27% (517), and 8% (145), respectively (Table 2). Munitions in the SG range of $2.5 \leq SG < 3$ (17%) were two times more likely to migrate ≤ 0.5 m compared to munitions with $SG < 2.5$ (8%) given similar forcing conditions. Migration percentages for the same SG values for "motion" munitions were 16% (57), 31% (108), 17% (61), 14% (47), 19% (65), and 3% (11). These percentages spread across the SG ranges, implying that SG may be less important for net migration provided the forcing is sufficient to exceed initiation of motion. Overall, 58% (202 of 349) of the net migration events were offshore directed. Wave non-linearity, the existence of an undertow, and local bed slope are factors that may relate to offshore migration.

Table 2. "No motion" and "motion" values and percentages based on the SG ranges.

SG Ranges	$2 \leq SG < 2.5$	$2.5 \leq SG < 3$	$3 \leq SG < 3.5$	$3.5 \leq SG < 4$	$4 \leq SG < 4.5$	$4.5 \leq SG < 5.8$	Total
No motion	8% (152)	17% (317)	19% (357)	21% (391)	27% (517)	8% (145)	1879
Motion	16% (57)	31% (108)	17% (61)	14% (47)	19% (65)	3% (11)	349

A net offshore or onshore migration distance magnitude exceeding 5 m was considered major and comprised 100 of 349 (29%) munitions. Of those 100 munitions, 67% (67) had SG of <3, implying that although SG values may be less important for "motion" migration provided the forcing is sufficient to exceed initiation of motion, the SG may become a dominant factor for long-distance migration. Migration distances showed no obvious trends with respect to the Shields number $\theta = \frac{\tau_b}{(\rho_s - \rho_w) g d_{50}}$ (Figure 9), where bed shear stress $\tau_b = \frac{1}{2}\rho_w f u^2$, f = friction factor, and ρ_s and ρ_w are sediment and fluid densities of 2650 kg/m^3 and 1000 kg/m^3, respectively, and commensurate with past studies showing a weak correlation between dimensionless parameters and migration distance [12,13,28]. However, small SG munitions (green symbols) clustered for $\theta < 5$ and corresponding greatest migration distances implying that the munitions with smaller SG may require weaker overall forcing for migration.

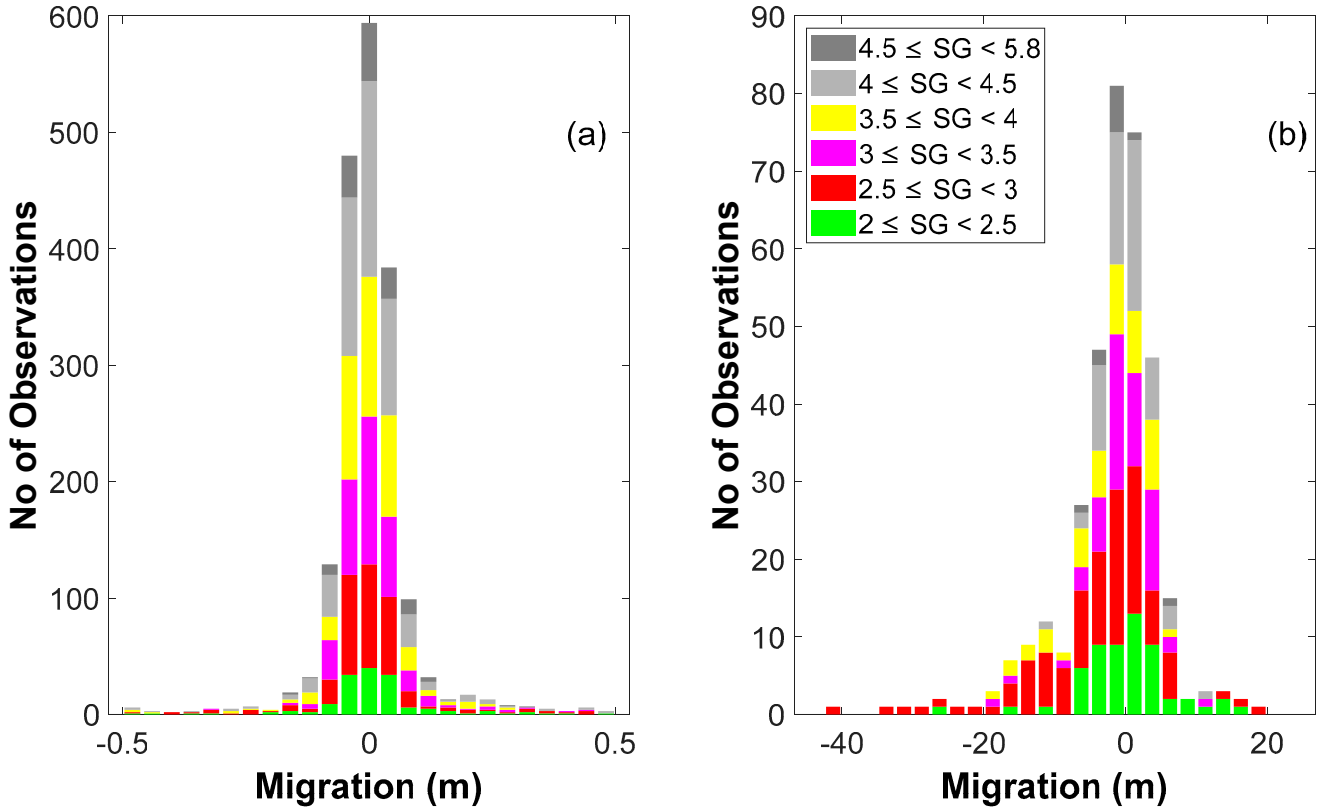

Figure 8. Migration distances for munitions in the nearshore; (**a**) no motion; (**b**) motion.

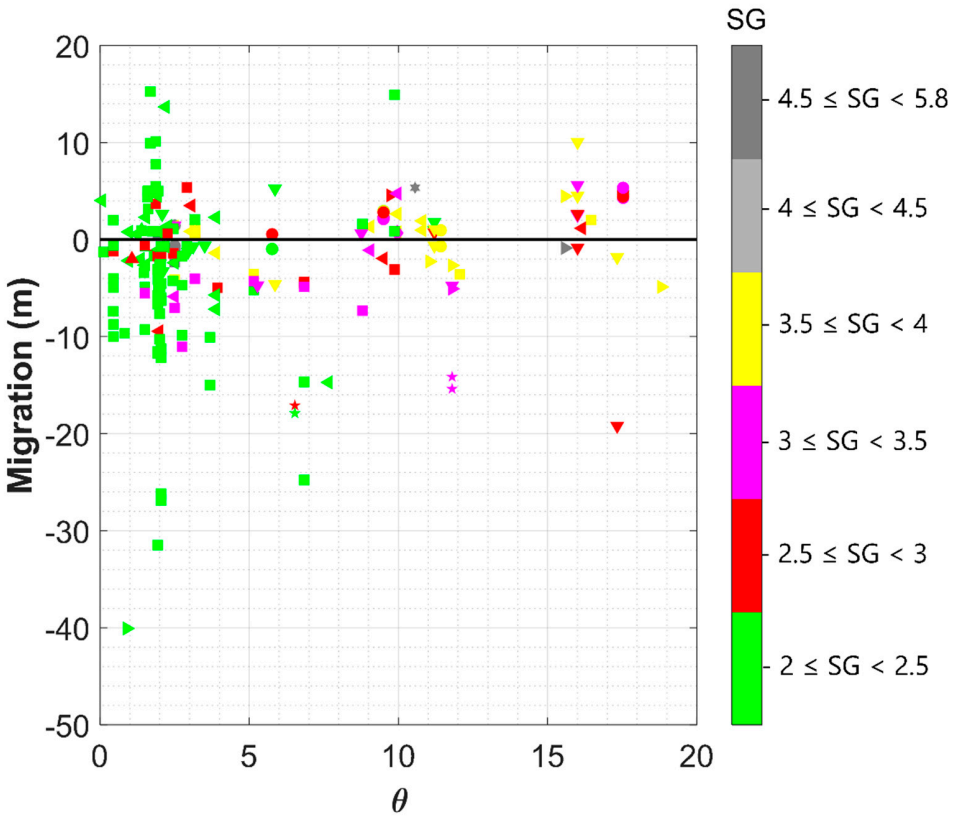

Figure 9. Migration as a function of Shields number for all motion observations. Positive and negative values represent onshore- and offshore-directed migrations, respectively. The shapes represent the Cases. Case01 to Case06 are ○, □, ▷, ◁, ▽, △, respectively.

4.2. Munitions Migration in the Offshore Zone

The offshore zone is defined as the region from $x = 0$ m to $x = 47$ m. It is characterized by flat bathymetry, continuous submergence of munitions, non-breaking waves, and minimal changes in the overall morphology. A total of 812 munition data points were obtained comprising 94% (764 of 812) and 6% (48 of 812) "no motion" and "motion" migrations, respectively (Table 3). There was a higher percentage (705 of 764; 92%) of the "no motion" munitions with SG $\geq$ 2.5. The corresponding "motion" (48; 6%) (Table 3a) implies that 60% (29) had SG < 2.5, while 83% (40) had SG < 3. In total, 31 of the 48 "motion" migrations had net onshore migration implying that more munitions (65%) migrated onshore in the offshore zone. Only 6 of 48 (13%) of the "motion" munitions traveled more than the 5 m cutoff for what is considered a major migration, and their SG values were all in the SG $2 \leq$ SG < 2.5 range. These observations suggest that in the offshore zone over flatter bathymetry, the munitions bulk density and wave skewness are important for net migration.

Table 3. "No motion" and "motion" values and percentages based on the SG ranges and cases (offshore).

(a) SG Ranges	**2 $\leq$ SG < 2.5**	**2.5 $\leq$ SG < 3**	**3 $\leq$ SG < 3.5**	**3.5 $\leq$ SG < 4**	**4 $\leq$ SG < 4.5**	**4.5 $\leq$ SG < 5.8**	**Total**
No motion	8% (59)	18% (141)	19% (146)	20% (151)	30% (231)	5% (36)	764
Motion	60% (29)	23% (11)	15% (7)	2% (1)	0%	0%	48
(b) Cases	**Case01**	**Case02**	**Case03**	**Case04**	**Case05**	**Case06**	**Total**
No motion	95% (112)	89% (131)	88% (99)	96% (139)	96% (178)	97% (105)	764
Motion	2% (2)	11% (16)	12% (13)	4% (6)	4% (8)	3% (3)	48
Total	114	147	112	145	186	108	812

The percentages in each case were calculated as a function of the total number of migration datapoints in the case (Table 3b). Case05 had the largest number of data points (186) because it contained more trials (10 trials) than the other cases (5 trials). Unsurprisingly, Case03, with the largest forcing combinations (Table 1), produced the largest percentage value for "motion" migration (12%) of all the cases (Table 3b). Case04 and Case05, produced nearly identical migration behavior for both "no motion" and "motion" migrations both at (96%, 4%), respectively (Table 3b). The histograms of the migrations in the offshore zone were separated into the cases (Figure 10). The "no motion" migrations across all of the cases follow a nearly normal distribution or are skewed towards onshore migration. The "motion" migrations across all cases skewed more towards the onshore (Figure 10). Expectedly, the SG values of the "motion" migrations were mostly in the $2 \leq$ SG < 2.5 and $2.5 \leq$ SG < 3 ranges, regardless of the case. Few "motion" munitions in the $3 \leq$ SG < 3.5 range (e.g., Figure 10, Case01, Case02, and Case03) migrated beyond 5 m, further emphasizing the importance of bulk density on munitions long-distance migration. As discussed in Section 3, the offshore zone experienced relatively weaker near-bed forcing due to the water depth (Figure 7).

4.3. Munitions Migration in the Surf Zone

The surf zone typically extended shoreward from $x = 47$ m to the surf/swash boundary between $x = 77$ m and $x = 97$ m, depending on the water depth and wave characteristics. This region was characterized by relatively steep slopes (1:20–1:5) with increasing steepness shoreward. Munitions in the surf zone accounted for 42–55% of the total munitions deployed and the migration observations in the surf zone account for 51% of the total migration data points. A total of 1212 surf zone observations from Case01 to Case06 were made comprising (241; 20%) and (971; 80%) data points for the "motion" and "no motion" net migrations, respectively (Table 4a). The 80% (971 of 1212) "no motion" net migrations observed in the surf zone were comparatively smaller than that of the offshore zone observations (94%). About 73% (713 of 971) of the munitions with "no motion" had

SG $\geq$ 3, implying that similar to the offshore zone, the "no motion" munitions tended to have higher density.

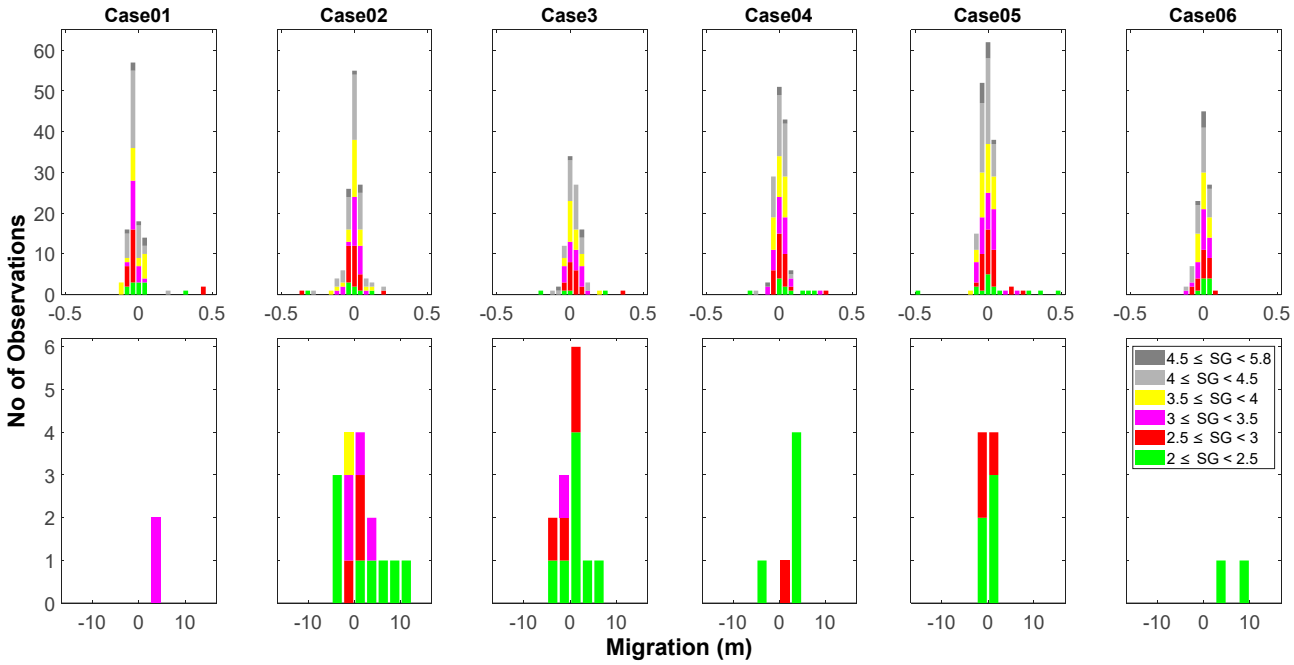

Figure 10. Migration distances for munitions in the offshore zone separated into cases. The top and bottom rows are the "no motion" and "motion" data for each case, respectively.

Table 4. "No motion and "motion" values and percentages based on the (a) SG ranges and (b) cases (surf).

(a) SG Ranges	**2 $\leq$ SG < 2.5**	**2.5 $\leq$ SG < 3**	**3 $\leq$ SG < 3.5**	**3.5 $\leq$ SG < 4**	**4 $\leq$ SG < 4.5**	**4.5 $\leq$ SG < 5.8**	**Total**
No motion	10% (93)	17% (165)	21% (200)	23% (222)	25% (246)	4% (45)	971
Motion	12% (28)	39% (93)	17% (40)	14% (34)	18% (43)	1% (3)	241
(b) Cases	**Case01**	**Case02**	**Case03**	**Case04**	**Case05**	**Case06**	**Total**
No motion	88% (144)	71% (174)	70% (106)	86% (171)	86% (221)	79% (155)	971
Motion	12% (19)	29% (72)	30% (46)	14% (27)	14% (35)	21% (42)	241
Total	163	246	152	198	256	197	1212

About 50% (120 of 241) of the "motion" munitions had SG < 3, as compared to the offshore zone, which had a value of 83%. About 34% (83 of 241) of the "motion" net migrations were greater than the 5 m cutoff for what was considered a major migration. Thirteen percent (11 of 83) and 49% (51 of 83) of the major migration observations were in the 2 $\leq$ SG < 2.5 and 2.5 $\leq$ SG < 3 ranges, jointly accounting for 60% of the munitions with net migrations greater than 5 m. The greatest net migration distances during the experiment were recorded in the surf zone with a maximum net migration distance of 40 m offshore (Figure 11, Case04). Net migration in the surf zone was predominantly offshore-directed 65% (157 of 241). This trend is in contrast with the offshore zone where net munitions migration was largely onshore-directed and may suggest the importance of gravity (slope) on munitions migration. However, the trend observed in the offshore zone persists in the surf zone, where Case03 had the relatively largest percentage of "motion" migration at 30% and the same migration pattern of (86%, 14%) for "no motion" and "motion" was observed for Case04 and Case05 (Table 4b).

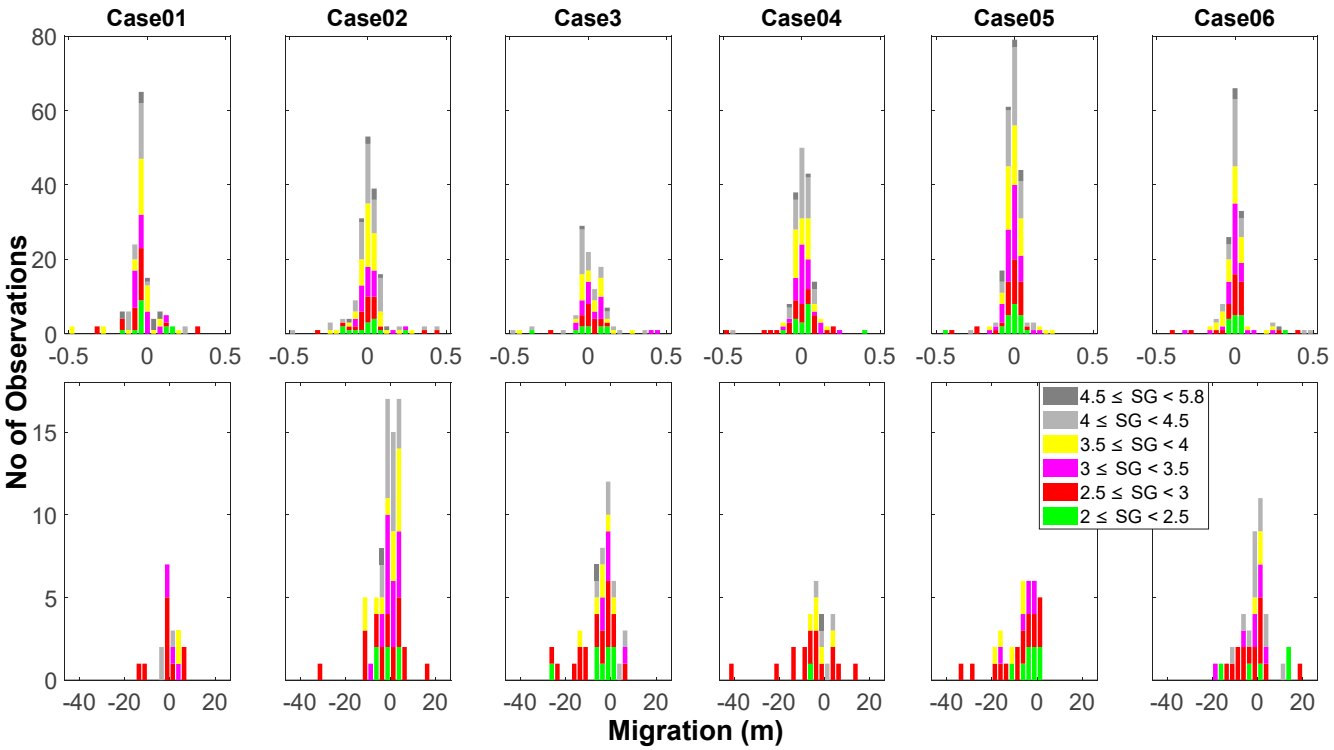

Figure 11. Migration distances for munitions in the surf zone separated into cases. The top and bottom rows are the "no motion" and "motion" data for each case, respectively.

The case-based migrations in the surf zone (Figure 11) had the "no motion" net migration following a nearly normal distribution and the "motion" net migrations left-skewed in favor of offshore migration. The "motion" exceptions are Case02, Case04, and Case06 with distributions more normal. The SGs of the "no motion" net migrations span the entire SG range from 2 to 5.8. A similar observation is made in the "motion" net migration, suggesting that hydrodynamics plays a more dominant role than munitions bulk density on migration in the surf zone, provided conditions are sufficient for migration to occur.

4.4. Munitions Migration in the Swash Zone

The swash zone extends from the farthest runup edge on the beach face to the surf/swash boundary. The boundary varied with trial from x = 77 m to x = 87 m due to the changing forcing conditions. The swash zone spans the shortest cross-shore distance of all three zones. The number of munitions initially deployed in the swash zone varied from 30 to 50 (19–32%) depending on the surf/swash boundary location. In addition to the exclusion of munitions that experienced no hydrodynamic forcing from the dataset, some munitions with significant offshore migration distances initially deployed in the swash zone ended up in the surf zone in subsequent trials. Such datasets were subsequently considered as part of the surf zone categorization.

There were 204 total observations in the swash zone which comprised 144 (71%) and 60 (29%) observations for "motion" and "no motion", respectively (Table 5a). Ninety-three percent (56 of 60) of the "motion" munitions had SG $\geq$ 3, suggesting that hydrodynamics and morphodynamics may play a more dominant role than density on munitions migration in the swash zone for energetic conditions. The maximum net onshore and net offshore migration distances were 12 m and 17 m, respectively (Figure 12, Case06). The percentages of the munitions migrations in either direction were similar with 47% (28 of 60) migrating offshore and 53% (32 of 60) migrating onshore. These swash zone observations for the "motion" munitions suggest a nearly equal probability of munitions migration in either direction, but the offshore-directed migrations are likely to migrate farther distances (Figure 12, Case06). The spread of the migration percentages and no observable trends be-

tween net migration distance and the SG for the "motion" munitions suggest that SG plays a lesser role in the "motion" munitions migration when forcing conditions are sufficient to cause migration.

Table 5. "No motion and "motion" values and percentages based on the SG ranges (swash).

(a) SG Ranges	**$2 \leq SG < 2.5$**	**$2.5 \leq SG < 3$**	**$3 \leq SG < 3.5$**	**$3.5 \leq SG < 4$**	**$4 \leq SG < 4.5$**	**$4.5 \leq SG < 5.8$**	**Total**
No motion	0% (0)	7.5% (11)	7.5% (11)	13% (18)	28% (40)	44% (64)	144
Motion	0% (0)	7% (4)	23% (14)	20% (12)	37% (22)	13% (8)	60
(b) Cases	**Case01**	**Case02**	**Case03**	**Case04**	**Case05**	**Case06**	**Total**
No motion	100% (2)	79% (46)	0% (0)	70% (23)	68% (60)	59% (13)	144
Motion	0% (0)	21% (12)	100% (1)	30% (10)	32% (28)	41% (9)	60
Total	2	58	1	33	88	22	204

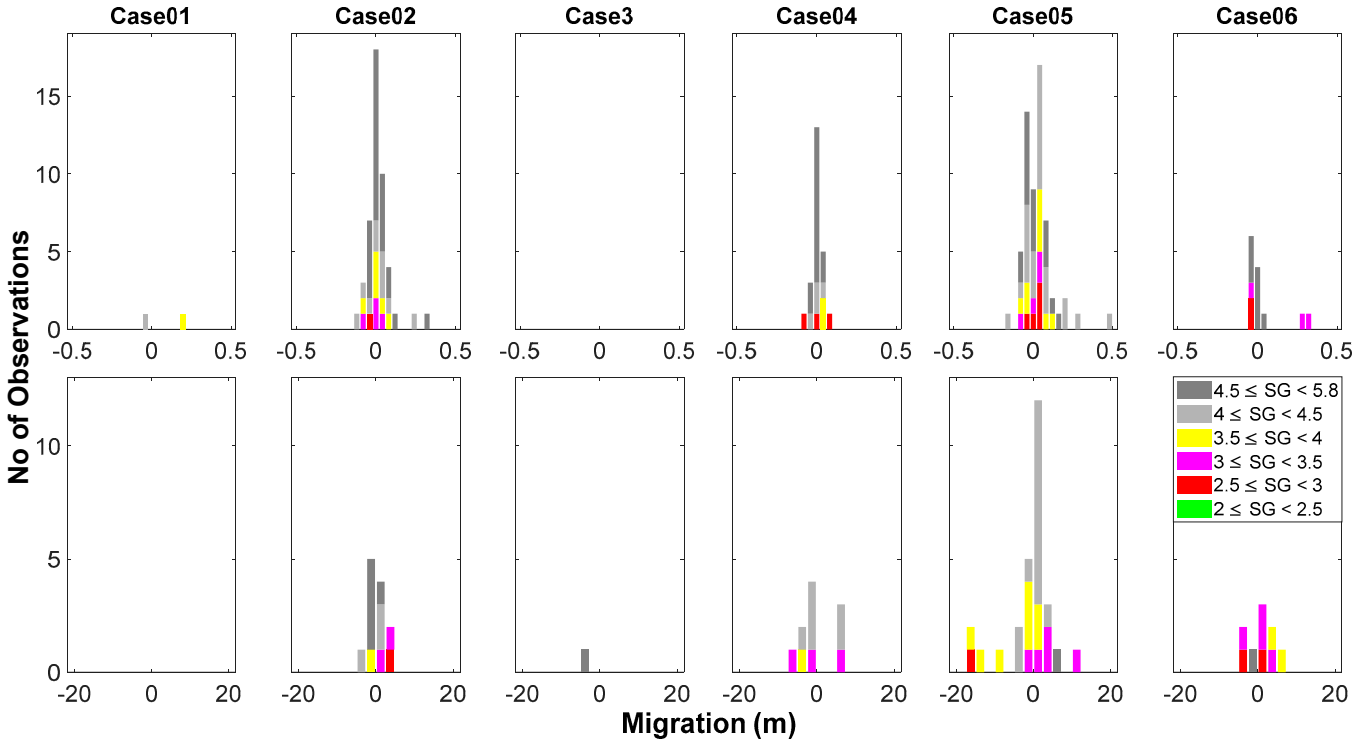

Figure 12. Migration distances for munitions in the swash zone separated into cases. The top and bottom rows are the "no motion" and "motion" data for each case, respectively.

The "no motion" munitions accounted for about 70% (144 of 204) of the swash zone observations. The increase in percentages with increasing SG indicates that denser munitions tend to experience "no motion" likely under weaker swash zone forcing. Approximately 92% of the "no motion" munitions had $SG \geq 3$, with the least dense munitions ($2 \leq SG < 2.5$) in the swash zone always migrating beyond 0.5 m. The $SG \geq 3$ munitions accounting for 92% of the "no motion" observations suggest that the threshold SG for motion/no-motion in the swash zone may be within the range of 2 to 3.

The "motion" and "no motion" observations in the swash zone appear contrasting. On one hand, munitions bulk density suggests that denser munitions tend to experience "no motion." On the other hand, SG seems to have minimal importance in the "motion" munitions, as there were no observable trends between net migration distance and the SG. The discrepancy between SG and migration in the "motion" and "no motion" datasets implies that SG is a key factor in the final determination of a munition experiencing

"motion" or "no motion", but the forcing is a more dominant driver of migration than the bulk density in munitions that experience significant net migration.

The swash zone had the smallest number of munitions observations of all three zones largely because of the migration of many initially proud munitions into the other zones and the relatively smaller area of intermittent swash motions. Case05 had a large number of data points due to the greater number of trials. The observed trend between Case04 and Case05 in the offshore and surf zones was also maintained in the swash zone (Table 5b). A similar pattern of (70%, 30%) and (68%, 32%) for "no motion" and "motion" migrations were observed in Case04 and Case05, respectively (Table 5b).

The offshore migration of the berm between x = 80 m and x = 90 m for most cases (Figure 7) explains the inability to locate some of the munitions initially placed in the swash zone of the SG value. Hence, only a few or no data points were observed for some of the cases (Figure 12). The few datapoints observed in Case01 were due to the swash extents being farther away from the shoreline, and hence many deployed munitions in the zone did not experience hydrodynamic forcing. Conversely, the strong forcing combination in Case03 which led to offshore migrations of most munitions initially deployed in the swash explains why (Figure 12, Case03) is nearly blank.

As with the surf zone, the SG distributions of both the "no motion" and "motion" net migrations spanned the entire SG range from 2 to 5.8, suggesting the relative importance of hydrodynamics over munitions bulk density.

4.5. IMU-Derived Munition Migration (Initiation of Motion)

The IMU data provided near-instantaneous observations of the munition migration in the surf zone. The interpretations of the observations with respect to the hydrodynamics and the beach slope in the vicinity of the munitions give insights into the complex interactions between munitions in the nearshore and the forcing conditions. The initiation of motion times of munitions at the same x = 82 m location relative to the start times of the wavemaker (t = 0 s) for cases with available data are presented in Table 6. The munition types are described in the following order: color—munition type, e.g., R81 implies Red 81 mm projectile (see Figure 3).

Table 6. Duration of time before initiation of motion due to the wave forcing relative to t = 0 s, the wave maker start time.

Experiment No	Munition Type, SG, and Initiation of Motion Time (s)		
Case02 Trial01	R81 (SG = 2.5) = 22.5	M81 (SG = 3.0) = 24.9	S81 (SG = 4.18) = 37.6
Case04 Trial01	R81 (SG = 2.5) = 87.4	No data	S81 (SG = 4.18) = 90.6
Case05 Trial01	M81 (SG = 3.0) = 12.1	Y81 (SG = 3.5) = 133.9	S81 (SG = 4.18) = 183.4
Case06 Trial01	R81 (SG = 2.5) = 45.6	No data	S81 (SG = 4.18) = 55.7

The wide-ranging time from forcing to "initiation of motion" (Table 6) was expected because the hydrodynamics of each case varied (Table 1). Across the cases shown, the less-dense instrumented R81 munition (SG = 2.5) consistently had shorter "initiation of motion" times than the instrumented S81 munition (SG = 4.18). This limited observation suggests that bulk density impacts the initiation of motion as less dense munitions of similar shapes and sizes are mobilized before the denser munitions originating from the same cross-shore position and under the same forcing. Conversely, overall hydrodynamics likely dominate over bulk density for munitions migration in the surf zone (Section 4.3) for long-distance migration.

The IMU data of a R81 munition (SG = 2.5) during Case02 Trial01 (h = 2.87, H_s = 1.1 m, T_p = 6 s) are presented to show the variability in the migration time history (Figure 13) where relative time (RTt) is referenced to a local time when the munition started to move. The overall duration of motion was about 31 min (1870 s). The munition trajectory was divided based on observations of change in migration behavior. Sections are numbered and color-coded (Figure 13) and examples include the change from offshore migration to roughly

stationary or roughly stationary to offshore migration. The beach profile (Figure 13b) and corresponding water level variation within 120 s of change in migration behavior (Figure 13c–j) are also shown. Free surface oscillations (η) were taken from the sensor closest to the midpoint of the migration range of the particular section. From relative time RTt = 0 s to RTt = 53 s, the munition migrated 5.61 m offshore (S1; blue) at a mean velocity of 0.11 m/s. Sections S2 (orange), S4 (purple), S6 (cyan), and S8 (black) have relatively similar properties where the munition experienced a series of small onshore/offshore motions, likely mimicking the flow oscillations. Net migrations were S2 (0.91 m), S4 (0.56 m), S6 (0.86 m), and S8 (2.08 m) over durations of 57 s, 87 s, 153 s, and 496 s, respectively. The corresponding cross-shore mean migration velocities range from 0.004 m/s to 0.016 m/s offshore. In S3 (yellow), a rapid offshore migration (2.19 m) was followed by a gradual onshore migration (2.01 m) and another rapid offshore migration (1.56 m) over ~325 s (RTt = 110 s to RTt = 435 s), resulting in net migration of 1.75 m offshore.

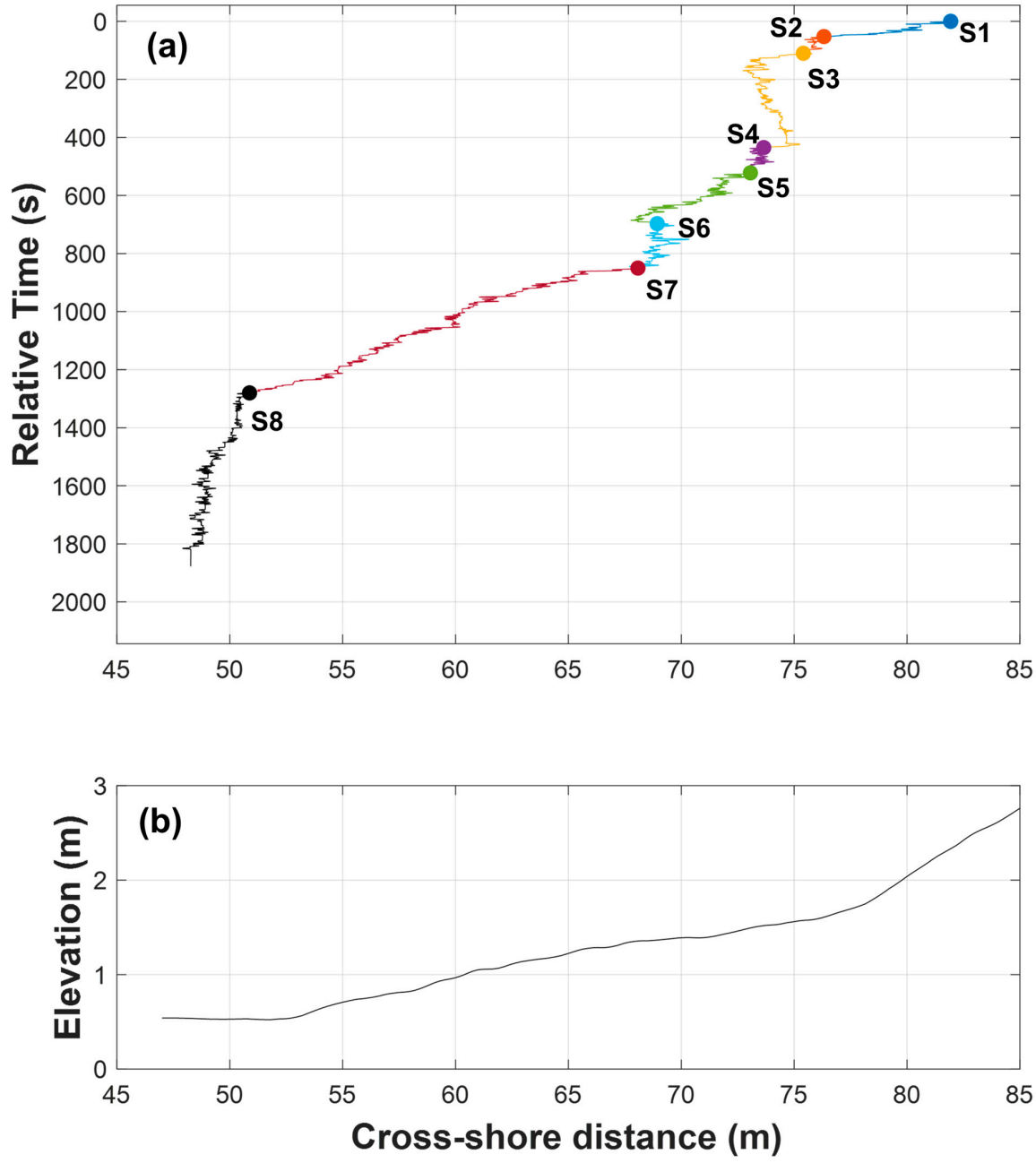

Figure 13. *Cont.*

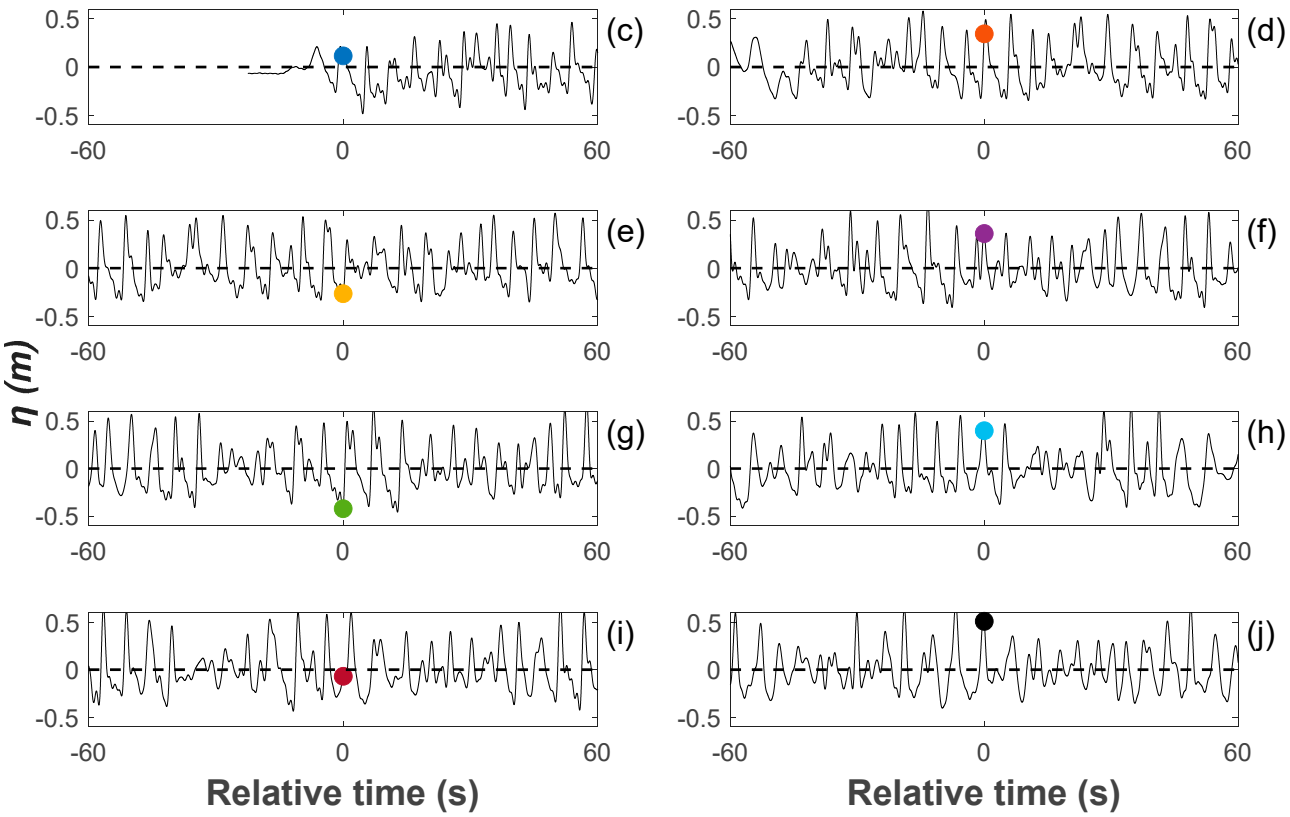

Figure 13. (**a**,**b**) The migration time history of an R81 (SG = 2.5) instrumented surrogate munition in the surf zone. Offshore migration is from right to left. The color changes depict the sectioning of the munition migration trajectory. The corresponding colored circles indicate the start of each migration section. (**b**) The beach profile for reference. (**c**–**j**) Free surface oscillations (η) 60 s before and after the onset of the S1 to S8 centered around a local RTt = 0 s. The colors correspond with the colors used for S1 to S8 in Figure 13a.

Conversely, S5 (green) from RTt = 522 s to $\underline{RTt}$ = 697 s initially started with onshore/offshore oscillations similar to S4 that led to a short net migration distance, then gradually migrated offshore before rapidly migrating back onshore in the last few seconds. The resulting mean migration velocity was 0.02 m/s. Section S7 (red) from $\underline{RTt}$ = 850 s to $\underline{RTt}$ = 1280 s experienced 17.20 m of offshore migration and a corresponding mean migration velocity of 0.04 m/s. These data show that munition migration varies considerably across the profile and with time of forcing.

Local hydrodynamics and bed slopes provide context for some of the tendencies of the behavior. The initiation of motion (S1) may have been triggered by a wave crest just before the start of a wave group, suggesting that the initial motion may not occur under the largest waves in the group. Transitions to S2, S5, S7, and S8 occurred inside wave groups with S2 and S8 initiated near wave crests, while S5 and S7 were initiated near wave troughs (Figure 13d,g,i,j). S3, S4, and S6 were initiated towards the end of a wave group with S3 near a trough, while S4 and S6 were near wave crests (Figure 13e,f,h). The different hydrodynamic conditions under which the sections were triggered suggest that changes in the behavior of munitions migration and trajectories are not tied solely to peak hydrodynamic conditions. Note that the discrepancies in the positions of the symbol on the waveforms in the subplots are due to the relative distances between the UDM sensors and the munitions locations. The rapid migration observed in S1 was likely aided by the local steep slope (1:8.5) between x = 76 m and x = 82 m. The observations in S2, S3, S4, and S5 from $\underline{RTt}$ = 53 s to $\underline{RTt}$ = 697 s coincide with a gentler beach slope (1:30) that had some portions characterized by local troughs or small negative slopes. Due

to the gentle slope, local hydrodynamics might have been more dominant in the three sections, but the gentle slope could have aided the observed onshore migration under skewed waves. In S7 (RTt = 850 s to $\underline{RTt}$ = 1280 s), the beach slope was steeper (1:17) from x = 53 m to x = 62 m, and the corresponding response on the munition migration was a burst of offshore migration over a relatively short time where the munition traveled 12 m offshore in 390 s (~890 to ~1280 s). From $\underline{RTt}$ = 1280 s to RTt = 1776 s, the munition entered the flat slope region from x = 53 m to the offshore. The migration speed and distance reduced, suggesting a dominant influence of the slope on the net migration. In the region, repeated onshore/offshore vacillation suggests that the munition may have been trapped in a local depression or developed a local scour hole, allowing for only restricted horizontal motions. The free surface oscillation observations (Figure 13c–j) may suggest more of a cumulative effect of the larger wave groups than the individual waves that led to the S1–S8 observations.

Deployed sensors were fixed in space, whereas the munition migration is Lagrangian. Thus, hydrodynamic statistics (Table 7) were calculated for the duration of the identified sections using the sensor located nearest the mean munition location. The local skewness (S_k) and asymmetry (A_s) were quantified from η [39] and expressed as

$$S_k = \frac{\langle \eta^3 \rangle}{\langle \eta^2 \rangle^{3/2}} \tag{1}$$

$$A_S = \frac{\left\langle H(\eta)^3 \right\rangle}{\langle \eta^2 \rangle^{3/2}}, \tag{2}$$

where H is the imaginary part of the Hilbert transform and < > denotes time averaging.

Table 7. Computed hydrodynamic parameters during each section of the migration.

Sections	UDM No	UDM Location (m)	H_s	S_k	A_S
S1	8	77	0.81	0.53	−0.03
S2	8	77	0.92	0.75	−0.60
S3	7	72	0.86	0.75	−0.51
S4	7	72	0.83	0.50	−0.41
S5	7	72	0.90	0.68	−0.29
S6	6	67	0.86	0.58	−0.48
S7	5	57	0.87	0.52	0.05
S8	3	47	0.83	0.79	0.06

An increase in wave non-linearity is denoted by wave skewness becoming more positive and asymmetry becoming more negative. Durations of nearly stationary motion (S2, S4, S6, and S8) have S_k ranging from 0.5 to 0.79, indicating that there is still moderate to strong onshore skewness; possibly balanced by profile slope. Corresponding asymmetries range from −0.6 to 0.06, indicating moderate asymmetry. The positive asymmetry in A_S may be due to the waveform adjusting as it came off the wave paddle. Offshore migration sections S1, S5, and S7 had S_k from 0.52 to 0.68 and A_S from −0.29 to 0.05. The onshore migration section, S3, had the second largest S_k of 0.75 and A_S of −0.51. These data suggest that wave skewness and asymmetry alone are insufficient to identify munition migration and/or migration direction.

The impact of bulk density on migration distance and duration was explored by comparing the three 81 mm munitions with SG = 2.5 (R81), SG = 3 (M81), and SG = 4.18 (S81) (Case02 Trial01, Figure 14). Marked differences were observed between the munitions: 1) The least dense R81 (SG = 2.5) had more observations (79) and the largest magnitudes of migration observations. The mean and standard deviation (std) values of the absolute motion distances were 0.53 m and 0.79 m, and 13 of the 14 absolute motion distances greater than 1 m across all three munitions were for R81 observations. 2) The most dense

S81 (SG = 4.18) had the fewest observations of motion (5) and the distance magnitudes (mean = 0.45, std = 0.29) were the smallest. 3) The moderate density M81 (SG = 3.0) experienced moderate motion events (7) and the mean and std values of the absolute motion distances were 0.47 m and 0.76 m. The mean values of the gross motions were R81 = 2.69 m, M81 = 0.92 m, and S81 = 1.03 m, as compared to the mean values of the net motions of R81 = 0.53 m, M81 = 0.47 m, and S81 = 0.45 m. These findings indicate the munitions are likely to oscillate onshore and offshore superimposed on a mean transport direction.

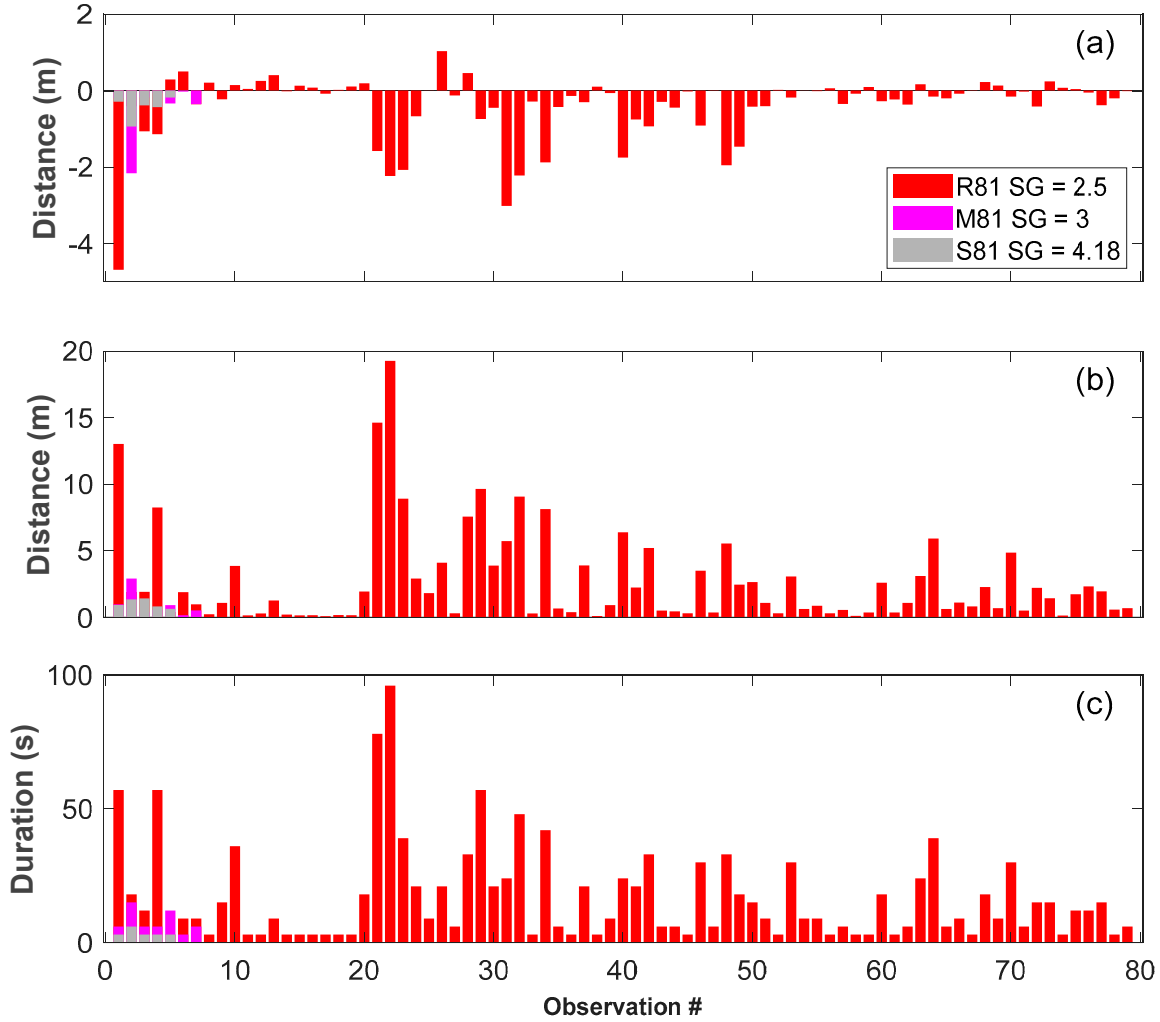

Figure 14. Migration distance as a function of observation of a 81 mm projectile with SG = 2.5 (R81), SG = 3.0 (M81), and SG = 4.18 (S81), (**a**) net migration, (**b**) gross migration, and (**c**) duration of the migration expressed in (**a**). Color coding is relative to Figure 3.

Offshore motions for the instrumented 81 mm munitions dominated regardless of SG with 100%, 100%, and 70% (55 of 79) of the R81, M81, and S18 events, respectively, being offshore-directed (Figure 14a). The corresponding durations of motion (Figure 14c) also show that the R81 was the most active, followed by the M81 and the S81. The most dense munition (S81) experienced the smallest "motion" durations with mean and std values of 3.6 s and 1.4 s, respectively (Figure 14c). The offshore dominance matches surf zone observations for the larger dataset (Figure 11) and further indicates the importance of beach slope on munitions migration.

5. Discussion

Net munitions migration in response to varying hydrodynamics provided aggregated quantification for a wide range of forcing combinations. The 84% "no motion" and 16%

"motion" migration observations across the beach profile were sub-divided as offshore (94% "no motion"; 6% "motion"), surf zone (80 "no motion"; 20% "motion"), and swash zone (71% "no motion"; 29% "motion"). Previous field studies on munitions mobility in wave-driven and tidal-current-dominated deeper water areas show that most munitions buried and/or remained in place after emplacement [7,9,12], commensurate with the present study indicating a dominance of no motion. However, when objects migrated, the probability of migration increased towards the shoreline. In the cases where forcing was sufficient for migration, there was a nearly equal chance of onshore or offshore migration in the swash zone, migration in the surf zone tended to be offshore-directed (65%, 157 of 241), while migration was onshore-dominant (65%, 31 of 48) in the offshore zone. The net migration distance varied with the shortest distances observed in the offshore zone and the largest in the surf zone. Similar migration trajectories were found in other studies of munitions migration where objects in the outer surf zone tended to migrate onshore [12] and those in the swash zone migrated onshore and offshore and were influenced by local slopes [13]. However, those in the surf zone showed no preferential direction in the study [13]. The flatter bathymetry and increased depth in the offshore zone may indicate that the wave orbital motion was insufficient to cause the migration of dense munitions. The skewed/asymmetric shape of waves in the intermediate water of the offshore zone coupled with the flat bathymetry may explain why more of the less dense munitions migrated onshore [40]. Wave-induced sediment transport, increased wave non-linearity, undertow, and steeper profile slopes in the surf and swash zones may also enhance or hinder munitions migration. The relatively long offshore migration distances in the surf zone may be attributed to the energetic wave shoaling and breaking conditions coupled with steeper slopes.

Swash zone flows are composed of two quasi-unidirectional components: uprush and backwash. Uprush flows originate from bore collapse and may provide enough force to cause onshore motion (against gravity). The munition or object elevation sometimes exceeds the berm elevation and becomes "trapped" in the depression between the berm and the dune. Forcing in this depression was generally not sufficient to cause further migration. In contrast, the munition or object may have migrated a short distance landward during uprush, but the backwash was sufficient (coupled with downslope gravity) to cause offshore migration. The importance of local beach slope to munitions migration was also identified in prior laboratory studies [13] and theoretical force balances [26,27]. The migration of munitions initially located on or close to the berm (x = 80 m and x = 90 m) in the swash into the surf zone coincided with the offshore migration of the berm observed in nearly all the cases. The SG of the munitions spanned a wide range, underpinning the dominant role of hydrodynamics and morphodynamics over munitions bulk density in the swash and surf zones. On the other hand, bulk density seemed to dominate over hydrodynamics and morphodynamics (weaker near-bed forcing and flat bathymetry) in the offshore zone.

Across the profile spanning the offshore, surf, and swash zones, munitions bulk density is important for long-distance net migration. In the offshore zone, munitions SG seemed to dominate over hydrodynamics, leading to 94% of munitions not migrating. In the surf zone, 73% of the "no motion" migrations had SG $\geq$ 3, implying that there may be an SG threshold separating when munitions in the nearshore migrate or mostly remain in place. The SG threshold for motion/no-motion is likely near SG = 2.5, close to the specific gravity of dry sand and matches field observations (SG < 2: "motion" and SG > 3: "no motion"; [12]) and prior discussions regarding the importance of SG for migration [7,41]. Additionally, the munition relative density $S_m = \frac{\rho_m}{\rho_s}$, can be used to differentiate between full mobility ($S_m < 1$), partial burial ($S_m \approx 1$), and full burial ($S_m > 1$) [42]. Similar-shaped S81 (SG = 4.18, $S_m = 1.58$) and R81 (SG = 2.5, $S_m = 0.94$) deployed in the surf zone (Table 6) align with these proposed ranges. At the start of Trial01 of Case02, the S81 ($S_m = 1.58$) initially migrated a short distance of about 3 m offshore within the first 250 s of forcing, and afterward became stationary buried in place. Conversely, a net offshore migration of 33.7 m

was observed for the R81 ($S_m = 0.94$) over the forcing duration of Case02 Trial01, with the munition remaining proud. The wide variability in the migration data (Figure 8) spanning the entire range of θ values from 0 to 20 reflects the difficulty associated with representing the stochastic behavior of migration with a deterministic model or dimensionless parameter. Thus, it is believed that a probabilistic model [32] for munitions migration will have better predictive success. For instance, the coupled Delft 3D-UnMES model site demonstration off the coast of a barrier island with an 81 mm mortar of SG 3 produced no migration, 0–5 m migration, and 5 m–50 m migration probabilities of 0.67–0.75, 0.94–0.99, and 0, respectively [32].

6. Conclusions

The migration of surrogate munitions and canonical objects was quantified in a large-scale wave flume over a mobile bed. The hydrodynamics consisted of six wave onsets of varying wave heights, periods, still water levels, and durations. The cross-shore profile was subdivided into the swash, surf, and offshore zones, where 152 surrogate munitions and canonical objects were deployed. Overall, 2228 migration measurements were recorded. Three instrumented munitions also provided near-instantaneous migration trajectories. Across all zones, 16% and 84% of the migration observations were classified as "motion" (net distance > 0.5 m) and "no motion" (net distance < 0.5 m), respectively. Similarly, the "motion" and "no motion" migration observations in the zones were offshore (6%; 94%), surf (20%; 80%), and swash (29%; 71%). The probability of munitions migration increased with proximity to the shoreline. There was a nearly equal chance of onshore or offshore migration in the swash zone. Migration in the surf zone tended to be offshore-directed (65%), while migration was onshore-dominant (65%) in the offshore zone.

Bulk density was the more dominant parameter for identifying migration in the offshore zone than the variations in hydrodynamics, and while the hydrodynamics and local slope were more important for munitions motion in the swash and surf zones, providing the forcing was sufficient to initiate motion. Bulk density was also found to impact the initiation of motion as inferred from instrumented munitions. Relating overall migration (Lagrangian) to fixed hydrodynamic measurements (Eulerian) was ineffective. Parameters such as the Shields number, wave skewness, and wave asymmetry estimated from the closest measurement location were insufficient to predict deterministically migration due to the observed wide scatter typical of the highly stochastic phenomena. Thus, it is anticipated that deterministic models of migration will struggle to achieve skill given the disparate nature of munitions response even under similar forcing, bulk density, and initial placement characteristics.

Author Contributions: Conceptualization, J.A.P., T.E.I., M.K.G. and J.S.; methodology, J.A.P., T.E.I. and E.C.; formal analysis, T.E.I., E.C. and J.A.P.; investigation, J.A.P., T.E.I., E.C., M.K.G. and J.S.; resources, J.A.P. and J.S.; data curation, T.E.I. and E.C.; writing—original draft preparation, T.E.I.; writing—review and editing, T.E.I., J.A.P., E.C., M.K.G. and J.S; visualization, T.E.I.; supervision, J.A.P., M.K.G. and J.S.; project administration, J.A.P. and J.S.; funding acquisition, J.A.P. All authors have read and agreed to the published version of the manuscript.

Funding: This work was supported by the Strategic Environmental Research and Development Program (SERDP) [grant number MR20-1094].

Institutional Review Board Statement: Not applicable.

Informed Consent Statement: Not applicable.

Data Availability Statement: The raw data supporting the conclusions of this article will be made available by the authors on request.

Acknowledgments: Authors would like to acknowledge the Strategic Environmental Research and Development Program (SERDP) for the funding. Additionally, the authors would like to thank Jonathan Harp (CHPT Manufacturing) for design support and fabrication of the surrogate munitions; Dominik Lapierre and Raky Rezgui for extensive technical assistance; Kelsey Fall, for guidance

during the data analysis stage; and Mackenzie Hammel, Christopher Lashley, Lillian Gilardi, David Bogart, Damien Pham-Van-Bang, Coralie Santerre, Sylvain Verrier, Juhee Ok, Ganga Caldera, Rodrigo Contreras, Eduardo Lopez Ramade, Nina Stark, Brendan Green, Katherine Anarde, Thomas Thelen, Po-Chen Chen, Cassie Everett, Ryan Mieras, Marie Pierre Delisle, and Ludivine Lafosse for volunteer assistance during the experiment. We thank three anonymous reviewers for comments improving the clarity of the paper.

Conflicts of Interest: Authors 2 and 3 were employed by the company Stantec and WSP, respectively. The remaining authors declare that the research was conducted in the absence of any commercial or financial relationships that could be construed as a potential conflict of interest.

References

1. Australian Government Defence. What Is Unexploded Ordnance (UXO). Available online: https://www.defence.gov.au/UXO/What/ (accessed on 2 May 2021).
2. Carton, G.; Jagusiewicz, A. Historic Disposal of Munitions in U.S. and European Coastal Waters, How Historic Information Can Be Used in Characterizing and Managing Risk. *Mar. Technol. Soc. J.* **2009**, *43*, 16–32. [CrossRef]
3. Wilkinson, I. Chemical Weapon Munitions Dumped at Sea: An Interactive Map. Available online: https://nonproliferation.org/chemical-weapon-munitions-dumped-at-sea/ (accessed on 27 February 2022).
4. SERDP. *Munitions in the Underwater Environment: State of the Science and Knowledge Gaps*; Environmental Security Technology Certification Program Office: Arlington, VA, USA, 2010.
5. US Army RDECOM. *Off-Shore Disposal of Chemical Agents and Weapons Conducted by the United States*; Aberdeen Proving Ground: Aberdeen, MD, USA, 2001.
6. Randall, K. A Real Ticking Time Bomb Recent Reports of Unexploded Bombs and Other Military Ordnance Washing up on the Florida Coast Could Pose Serious Threats. Available online: https://shorturl.at/aqxD6 (accessed on 8 November 2023).
7. Calantoni, J.; Staples, T.; Sheremet, A. *Long Time Series Measurements of Munitions Mobility in the Wave-Current Boundary Layer*; SERDP Project Number 2320 Joseph Calantoni Report Number; DTIC: Fort Belvoir, VA, USA, 2014.
8. Garcia, M.H.; Landry, B.J. *Large-Scale Laboratory Experiments of Incipient Motion, Transport, and Fate of Underwater Munitions Under Waves, Currents, and Combined-Flows*; University of Illinois: Champaign, IL, USA, 2018.
9. Klammler, H.; Sheremet, A.; Calantoni, J. Seafloor Burial of Surrogate Unexploded Ordnance by Wave-Induced Sediment Instability. *IEEE J. Ocean. Eng.* **2020**, *45*, 927–936. [CrossRef]
10. Rennie, S.E.; Brandt, A.; Friedrichs, C.T. Initiation of Motion and Scour Burial of Objects Underwater. *Ocean. Eng.* **2017**, *131*, 282–294. [CrossRef]
11. Bruder, B.; Cristaudo, D.; Puleo, J.A. Smart Surrogate Munitions for Nearshore Unexploded Ordnance Mobility/Burial Studies. *IEEE J. Ocean. Eng.* **2018**, *45*, 284–303. [CrossRef]
12. Traykovski, P.; Austin, T. *Continuous Monitoring of Mobility, Burial and Re-Exposure of Underwater Munitions in Energetic Near-Shore Environments*; Woods Hole Oceanographic Institution: Alexandria, VA, USA, 2017.
13. Cristaudo, D.; Puleo, J.A. Observation of Munitions Migration and Burial in the Swash and Breaker Zones. *Ocean. Eng.* **2020**, *205*, 107322. [CrossRef]
14. Voropayev, S.I.; Testik, F.Y.; Fernando, H.J.S.; Boyer, D.L. Burial and Scour around Short Cylinder under Progressive Shoaling Waves. *Ocean. Eng.* **2003**, *30*, 1647–1667. [CrossRef]
15. Gross, B.M. Mobility of unexploded ordnance using spherical surrogates in the swash zone, Thesis. 2019. Available online: http://udspace.udel.edu/handle/19716/25065 (accessed on 27 February 2022).
16. Idowu, T.; Gangadharan, M.; Chapman, E.; Stolle, J.; Pham van Bang, D.; Puleo, J. Behavior of Variable Density Munitions Under Dam Break Forcing. *Coast. Eng. Proc.* **2023**, *37*, 123. [CrossRef]
17. Luccio, P.A.; Voropayev, S.I.; Fernando, H.J.S.; Boyer, D.L.; Houston, W.N. The Motion of Cobbles in the Swash Zone on an Impermeable Slope. *Coast. Eng.* **1998**, *33*, 41–60. [CrossRef]
18. Wengrove, M.; Garcia-Medina, G. *Munition Mobility in Mixed Grain (Sand, Gravel, Cobble) Environments*; Oregon State University: Corvallis, OR, USA, 2022.
19. Cataño-Lopera, Y.A.; Demir, S.T.; García, M.H. Self-Burial of Short Cylinders under Oscillatory Flows and Combined Waves plus Currents. *IEEE J. Ocean. Eng.* **2007**, *32*, 191–203. [CrossRef]
20. Demir, S.T.; García, M.H. Experimental Studies on Burial of Finite-Length Cylinders under Oscillatory Flow. *J. Waterw. Port Coast. Ocean Eng.* **2007**, *133*, 117–124. [CrossRef]
21. Friedrichs, C.T.; Rennie, S.E.; Brandt, A. Self-Burial of Objects on Sandy Beds by Scour: A Synthesis of Observations. In Proceedings of the 8th International Conference on Scour and Erosion, ICSE 2016, Oxford, UK, 12–15 September 2016; pp. 179–189. [CrossRef]
22. Breslin, S. Ordnance Found Washed Up on Outer Banks Beaches as Hurricane Maria Churns Up Sea. Available online: https://weather.com/news/news/outer-banks-beaches-ordnance-found-north-carolina (accessed on 20 February 2024).
23. Geib, C. Tracking Unexploded Munitions Long-Buried Ordnance Lingers on U.S. Coasts. Available online: https://www.whoi.edu/oceanus/feature/tracking-uxos/ (accessed on 5 May 2021).

24. Parry, W. A Century After WWI, Munitions Still Making Way onto Beaches. Available online: https://apnews.com/article/cca295bd3bb547ec96b79c561c134ff0 (accessed on 4 May 2021).
25. Puleo, J.A.; Calantoni, J. *SERDP Workshop on UXO Mobility, Burial, and Exposure Processes: Discussion for a Demonstration Project*; University of Delaware: Newark, DE, USA, 2023.
26. Chu, P.C. *Coupled Ensemble Seafloor Environment and 6-DOF (CESE6D) Model for Assessing Characteristics of Munitions Underwater and Their Environment*; US Strategic Environmental Research and Development Program: Alexandra, VA, USA, 2023.
27. Cristaudo, D.; Gross, B.M.; Puleo, J.A. Momentum Balance Analysis of Spherical Objects and Long-Term Field Observations of Unexploded Ordnance (UXO) in the Swash Zone. *J. Mar. Sci. Eng.* **2023**, *11*, 79. [CrossRef]
28. Friedrichs, C.T.; Rennie, S.E.; Brandt, A.; Sarah, E. *Simple Parameterized Models for Predicting Mobility, Burial and Re-Exposure of Underwater Munitions*; SERDP Final Report MR-2224; Virginia Institute of Marine Science, William & Mary: Gloucester Point, VA, USA, 2018. [CrossRef]
29. Hsu, T.-J.; Tsai, B.; Tarazouj, A.S.; Chauchat, J.; Montella, E.P.; Bonamy, C. Novel Eulerian Two-Phase Simulations for Burial Dynamics of Munitions Phase I. 2020. Available online: https://serdp-estcp.mil/projects/details/143e9c49-ab38-4d63-a32c-c2a2805de64f/mr20-1478-project-overview (accessed on 27 February 2022).
30. Liu, X.; Qiu, T. *INTERIM REPORT. Three-Dimensional Computational Modeling of Turbulent Flow Field, Bed Morphodynamics and Liquefaction Adjacent to Munitions*; The Pennsylvania State University: University Park, PA, USA, 2019.
31. Rennie, S. *Underwater Munitions Expert System to Predict Mobility and Burial*; Johns Hopkins Applied Physics Laboratory: Laurel, MD, USA, 2017.
32. Palmsten, M.L.; Penko, A.M. *Probabilistic Environmental Modeling System for Munitions Mobility SERDP Project Number MR-2733*; U.S. Naval Research Laboratory: Washington, DC, USA, 2020.
33. Rennie, S.; Brandt, A.; Ligo, J.G. *Underwater Munitions Expert System for Remediation Guidance Prototype Underwater Munitions Expert System: Demonstration and User Guide*; Johns Hopkins University: Baltimore, MD, USA, 2019.
34. Penko, A. Munitions Response Library for Site Management. Available online: https://serdp-estcp.mil/projects/details/fc62c019-c1de-46f5-9542-5a1d785fc910/mr21-5207-project-overview (accessed on 4 June 2024).
35. LHE Large Scale Wave Flume. Available online: https://lhe.ete.inrs.ca/wp-content/uploads/2020/04/LHE_Flyer_2020.pdf (accessed on 6 March 2021).
36. Hughes, S.A. *The TMA Shallow-Water Spectrum Description and Applications (CERC-84-7)*, Washington, DC, USA, 1984.
37. Frank, D.; Landry, B.J.; Calantoni, J. Investigating Munitions Mobility in Oscillatory Flows with Inertial Measurement Units. In Proceedings of the OCEANS 2016 MTS/IEEE Monterey, Monterey, CA, USA, 19–23 September 2016.
38. Baldock, T. *Swash Zone Dynamics BT—Encyclopedia of Coastal Science*; Finkl, C.W., Makowski, C., Eds.; Springer International Publishing: Cham, Switzerland, 2019; pp. 1664–1674. ISBN 978-3-319-93806-6.
39. Elgar, S.; Guza, R.T. Nonlinear Model Predictions of Bispectra of Shoaling Surface Gravity Waves. *J. Fluid Mech.* **1986**, *167*, 1–18. [CrossRef]
40. NAVFAC. *Hydrodynamic Mobility Analysis of UXO Transport Andrew Bay Adak, Alaska*; Department of Navy: Adak, AK, USA, 2013.
41. Calantoni, J. *Informal Workshop on Burial and Mobility Modeling of Munitions in the Underwater Environment*; SERDP and ESTCP Office: Alexandria, VA, USA, 2014.
42. Calantoni, J. Long Time Series Measurements of Munitions Mobility in the Wave-Current Boundary Layer SERDP Project Number 2320. Available online: https://www.naoc.org/_cache/files/b/f/bf9ce668-450c-4abe-85b8-f4d3e424980b/F4E8E00F76C5FE0661B1923B1DDFB4EB.mr-2320-calantoni.pdf (accessed on 6 June 2024).